

1    **DATA REPOSITORY**

2

3    **Analytical methods**

4    ***Mineral Separation***

5    Samples (5 to ~50 kg) were jaw-crushed and disk-milled to <420  $\mu\text{m}$  and heavy mineral  
6    concentrates prepared using a Gemini table, heavy liquids (methylene iodide) and Frantz LB-  
7    1 separator. Grains selected for LA-ICPMS were mounted in epoxy blocks and imaged in  
8    BSE and CL modes by SEM prior to analysis by Dr. S. Parry and Mr. G. Turner of the British  
9    Geological Survey.

10

11    ***Laser ablation ICP-MS***

12    Laser ablation data were obtained on a Nu Instruments multiple collector inductively coupled  
13    plasma mass spectrometer (MC-ICP-MS). The NIGL Nu MC-ICP-MS collector block  
14    permits simultaneous collection of masses relevant to U-Pb chronology (masses 202 through  
15    207, 235, and 238). Further details are given for an almost identical collector configuration  
16    by Simonetti et al. (2005). Data collection, reduction and propagation of uncertainties follow  
17    Horstwood et al. (2003) and Bauer et al. (2011). Discrete dynode secondary electron  
18    multipliers were used to measure  $^{204}\text{Pb}+^{204}\text{Hg}$ ,  $^{206}\text{Pb}$  and  $^{207}\text{Pb}$ , with other isotopes of interest  
19    measured on Faraday cups. Targeted zircons were sampled using a New Wave Research  
20    UP193-FX 193 nm ArF excimer laser microprobe system. Zircons were ablated for 20  
21    seconds using a 25  $\mu\text{m}$  static spot at a laser fluence of ca. 2.5  $\text{J cm}^{-2}$ . These ablation  
22    protocols provided reconnaissance level data with  $^{206}\text{Pb}/^{238}\text{U}$  ratio uncertainties generally  
23    <2%. Instrumental mass fractionation was monitored using a mixed natural Tl- $^{235}\text{U}$  solution  
24    introduced via a Nu Instruments DSN 100 desolvating nebulizer. Fractionation related to  
25    laser ablation was corrected in unknowns by analyzing zircon reference materials. During the

26 course of this study the following zircon standards were used: 91500 dated at  $1062.4 \pm 0.4$   
27 Ma (Wiedenbeck et al., 1995), GJ-1 dated at  $600.4 \pm 0.6$  Ma, (Jackson et al., 2004) and 602.3  
28  $\pm 1$  Ma (current value from NIGL TIMS data using the EARTHTIME  $^{205}\text{Pb}$ - $^{233}\text{U}$ - $^{235}\text{U}$  tracer),  
29 and the  $337.33 \pm 0.38$  Ma Plesovice zircon (Sláma et al., 2008). Raw data was reduced using  
30 an in-house Excel data reduction worksheet. Given the reconnaissance nature of the LA-ICP-  
31 MS analytical work, data with <10% discordance were accepted for age calculations where  
32 the contaminant was deemed most likely to be common Pb from the abundant melt inclusions  
33 in many of the zircons (see DR Fig 2). Zircon data were rejected in instances where mixing  
34 was along obvious <3000 Ma – non-zero discordia lines, and grains where sufficient common  
35 Pb was present to result in >10% discordance.

36

37 ***U-Pb (zircon) Chemical Abrasion Isotope Dilution Thermal Ionisation Mass Spectrometry***  
38 ***(CA-ID-TIMS)***

39 Zircons analysed by TIMS were subjected to “chemical abrasion” (thermal annealing and  
40 subsequent leaching pre-treatment; Mattinson, 2005) to effectively eliminate Pb-loss. Zircons  
41 were heated in a muffle furnace at  $900 \pm 20^\circ\text{C}$  for ~60 hours in quartz beakers before being  
42 transferred to 3 ml Hex Savillex beakers, which were in turn placed in a Parr vessel, and  
43 leached in a ~5:1 mix of 29M HF + 30% HNO<sub>3</sub> for 12 hours at ~180°C. The acid solution  
44 was removed, fractions rinsed in ultrapure H<sub>2</sub>O, fluxed on a hotplate at ~80°C for 1 hr in 6 M  
45 HCl, ultrasonically cleaned for 1 hr, and then placed back on the hotplate for an additional 30  
46 min. The HCl solution was removed and the fractions (single zircon crystals or a single  
47 fragment) were selected, photographed (in transmitted light) and again rinsed (in ultrapure  
48 acetone) prior to being transferred to 300 µl Teflon PFA microcapsules and spiked with the  
49 mixed EARTHTIME  $^{233}\text{U}$ - $^{235}\text{U}$ - $^{205}\text{Pb}$  tracer. The single zircons or fragments were dissolved  
50 in ~ 120 µl of 29 M HF with a trace amount of 30% HNO<sub>3</sub> at ~220°C for 48 hours, with the

51 microcapsules housed within Parr vessels. The zircon digests were subsequently dried to  
52 fluorides and then converted to chlorides in 3M HCl at ~180°C overnight. U and Pb were  
53 separated using standard HCl-based anion-exchange chromatographic procedures on 0.05 ml  
54 PTFE columns manufactured in-house (Corfu and Noble, 1992). Isotope ratios were  
55 measured using NIGL's Thermo-Electron Triton Thermal Ionisation Mass-Spectrometer  
56 (TIMS) dedicated to low-blank U-Pb geochronology (Triton 2). Pb and U were loaded  
57 together on a single Re filament in a silica-gel/phosphoric acid mixture (Gerstenberger and  
58 Haase, 1997). Pb isotopes were measured by peak-hopping on a single SEM detector. U  
59 isotope measurements were made in static Faraday mode. Age calculations and uncertainty  
60 estimation (including U/Th disequilibrium) were based upon the algorithms of Schmitz and  
61 Schoene (2007). All acids were prepared by sub-boiling distillation: HCl and HNO<sub>3</sub> were  
62 double-distilled in quartz and HF was double-distilled in Teflon. Ultrapure water with a  
63 resistivity of 18 MΩ was prepared with a Milli-Q system. All reagents were blank-checked  
64 prior to use.

65 <sup>206</sup>Pb/<sup>238</sup>U dates are calculated using the <sup>238</sup>U and <sup>235</sup>U decay constants of Jaffey et al.  
66 (1971) and corrected for initial U/Th disequilibrium using an assumed magma Th/U ratio of  
67 4, typical for magmatic systems. A value of <sup>238</sup>U/<sup>235</sup>U<sub>zircon</sub> = 137.818 ± 0.045 (Hiess et al.,  
68 2012) was used in the data reduction calculations. Compared to calculations using the old  
69 'consensus' value (<sup>238</sup>U/<sup>235</sup>U = 137.88) this has the effect of reducing <sup>207</sup>Pb/<sup>206</sup>Pb dates by ca.  
70 0.98 Myr at the age range of interest (ca. 560 to 620 Ma) and reduces the <sup>206</sup>Pb/<sup>238</sup>U dates by  
71 <5 kyr. For U–Pb dates of this age, the <sup>206</sup>Pb/<sup>238</sup>U dates are the most precise and robust. In  
72 contrast, the <sup>207</sup>Pb-based dates (<sup>207</sup>Pb/<sup>235</sup>U and <sup>206</sup>Pb/<sup>207</sup>Pb) are considerably less precise and  
73 hence are only used to assess concordance of the U–Pb (zircon) systematics.

74

75

76    **Detailed geochronology sample descriptions**

77    ***Blackbrook Group***

78    Three Blackbrook Group samples were examined in this study. Sample JNC 916 was  
79    collected at Morley Quarry (BNG SK 4766 1787) from a several meters-thick succession of  
80    volcanioclastic sandstones, siltstones and mudstones, just above the exposed base of the Ives  
81    Head Formation. At Morley Quarry, individual graded units (Bouma A-E divisions) typically  
82    commence in structureless, very coarse-grained volcanioclastic sandstone in which are  
83    embedded sporadic angular fragments of laminated volcanioclastic siltstone ripped up from the  
84    underlying beds. They show an upward transition into medium-grained sandstone, which in  
85    turn develops a diffuse parallel-stratification before passing up to parallel-laminated siltstone  
86    and mudstone. An outstanding petrographical feature of JNC 916 is the general uniformity of  
87    the angular to subrounded dacitic volcanic grains, which enclose small quartz and plagioclase  
88    phenocrysts; their groundmasses are extremely fine-grained and microcrystalline although  
89    some show a slightly coarser, microgranular texture. Plagioclase and quartz also occur as  
90    discrete, fragmented euhedra between the lithic grains. This graded bed is comparable to the  
91    ‘secondary monomagmatic volcanioclastic turbidites’ of Schneider et al. (2001) which show  
92    mild reworking and clast heterogeneity.

93              JNC 836 was sampled (BNG SK 4772 1700) from the middle part of a 2.5 m thick  
94    volcanioclastic turbidite (see Fig. 3a of Carney, 1999). The position of this turbidite is critical  
95    in terms of palaeontology, since its uppermost bedding plane contains impressions of  
96    *Ivesheadia*, *Blackbrookia* and *Shepsheadia* (Boynton and Ford, 1995; Liu et al., 2011). Sand-  
97    size, angular to subrounded volcanic grains predominate in this sample. These grains are  
98    remarkably homogeneous with ~85 per cent having uniformly microcrystalline groundmasses  
99    and the remainder exhibiting varying degrees of patchy coarsening to microgranular or faintly  
100   spherulitic textures truncated at grain edges (DR Fig. 1a). Many grains contain quartz  
101   microphenocrysts indicating a dacitic composition for the parental magmas; one grain was

102 also seen to contain a euhedral, acicular zircon crystal. Sharply angular to locally subhedral  
103 quartz and plagioclase phenocryst fragments are particularly common within the matrix to the  
104 lithic grains. These petrographic characteristics strongly resemble those of JNC 916 and thus  
105 JNC 836 is interpreted to have had a similar origin.

106 JNC 917 is from the South Quarry Breccia Member located about 600 m  
107 stratigraphically above the other two samples. The sample was obtained from the South  
108 Quarry type locality (BNG SK 4637 1712). Exposed faces in the quarry consist of a few  
109 meters of stratified to massive coarse-grained volcaniclastic sandstone, passing upwards into  
110 a breccia with large contorted rafts of laminated mudstone embedded in a volcaniclastic  
111 sandstone matrix. In thin section, the analysed sample contains about 50-60% plagioclase and  
112 quartz, present as phenocrysts in dacitic lithic volcanic grains, or as fragmented to partially-  
113 fragmented crystals concentrated within the matrix between the grains. Lithic grains show a  
114 range of crystallinities from exceedingly fine-grained, virtually aphanitic, to more coarsely  
115 crystalline varieties with microgranular textures. Patchy recrystallization is commonly seen  
116 within the confines of a single grain (DR Fig. 1b). Some lithic grains contain very large  
117 embayed quartz euhedra surrounded by a thin ‘skin’ consisting of the microcrystalline matrix.  
118 In other outcrops, a degree of heterogeneity is shown by the lithic volcanic grains, and some  
119 examples possess a perlitic texture (Carney, 1994). The sedimentary features of the South  
120 Quarry Member are consistent with a history of secondary reworking involving submarine  
121 slumping of incompletely consolidated volcaniclastic strata.

122 ***Maplewell Group***

123 The oldest sample in the Maplewell Group to yield dateable zircons is JNC 918 from the  
124 Benscliffe Breccia, a highly distinctive unit at the base of the Beacon Hill Formation (Fig. 1).  
125 Sample JNC 918 was collected from the Benscliffe Breccia Member at the ‘Pillar Rock’ type  
126 locality in Benscliffe Wood (BNG SK 5146 1246). These exposures show 3+ meters of  
127 massive breccia in which lapilli- to small block-size fragments of andesite are set in a poorly

128 sorted matrix of crystal-rich, coarse-grained volcaniclastic sandstone (see Fig. 3b of Carney,  
129 1999). The andesite lapilli and blocks are angular to subrounded, with rather diffuse margins  
130 when viewed in polished slabs, with only limited petrographic variation. Many have coarsely  
131 microgranular textures, but some possess local areas containing small, stubby plagioclase  
132 laths with random orientation. A minor proportion of the lapilli and blocks have finely  
133 microcrystalline texture. In some of the larger andesitic blocks the degree of crystallinity  
134 decreases outwards to rims of finely microcrystalline material which, as with the exposed  
135 rock surfaces, are somewhat poorly defined against the matrix. When compared with the  
136 andesite fragments, the matrix is notably enriched in plagioclase and quartz crystals (DR Fig.  
137 1c); these are small and most are shattered and/or fragmented, appearing to have been  
138 granulated during their entrainment between the andesite blocks. The essentially  
139 monolithological nature of the andesite fragments would satisfy the criterion of Stix (1991)  
140 for a primary mass flow of pyroclastic debris, and the unit was interpreted by Carney (1999)  
141 as a long-runout subaqueous pyroclastic block flow marking a major eruptive event at the  
142 base of the Maplewell Group.

143 Volcaniclastic strata from the western flank of the Charnwood anticlinal structure  
144 were sampled (JNC 907) in the southern part of Bardon Hill Quarry (BNG SK 4572 1289)  
145 from a well-bedded volcaniclastic sequence faulted against the Bardon Hill Volcanic  
146 Complex. On the basis of regional correlations, it was originally thought that this sequence  
147 was from the middle part of the Bradgate Formation. Correlation with horizons sitting close  
148 to the base of the Beacon Hill Formation (Fig. 2), however, is equally likely based on our  
149 further mapping and is our preferred interpretation. Zircons were extracted from ca. 20 kg  
150 bulk sample of normally graded volcaniclastic siltstones and sandstones showing varying  
151 degrees of coarseness and bedding. In thin section, the sampled coarse grey-green  
152 volcaniclastic sandstone contains abundant angular quartz and plagioclase crystal fragments,  
153 although the dominant constituents are tightly packed subrounded to highly angular lithic

154 volcanic grains. These are heterogeneous in terms of their lithology with some consisting of  
155 peripherally ragged fragments of oxidised andesite and locally with spherulitic and shardic  
156 textures. Most of the fragments are andesite or low-silica dacite, with textures ranging from  
157 aphanitic to microgranular and fluxional/intergranular.

158 Sample JNC 911 was collected from the summit of Beacon Hill (BNC SK 5091 1488)  
159 and is the type locality for the Beacon Tuff Member of the Beacon Hill Formation (Moseley  
160 and Ford, 1985). The Beacon Hill tuffs are typically siliceous with a flinty appearance, and  
161 are generally fine- to medium-grained and laminated; some intervals show large-scale load  
162 structures (Carney, 2000b). In thin section, vitric shards are concentrated within silty laminae  
163 and the larger examples show blocky, sliver and y-shapes and internal replacement by grainy  
164 amorphous material. The matrix between the shards, and dominating laminae devoid of such  
165 shards, consists of exceedingly fine grained microcrystalline quartzo-feldspathic material.  
166 Abundant but faint and shadowy shardic outlines and bubble-wall textures are visible in this  
167 microcrystalline material and is interpreted here as finely comminuted ash. These tuffs  
168 probably originated as primary fall-out from ash clouds followed by settling out through the  
169 water column to the sea-floor.

170 The overlying Bradgate Formation is dated by the only sample out of several  
171 collected from this formation that yielded datable zircons (JNC 912), from the ‘Park Breccia’  
172 unit at the base of the Bradgate Formation. This unit (Worssam and Old, 1988) denotes a  
173 particularly prominent sedimentary breccia horizon that typically occurs a few to several  
174 meters below the Sliding Stone Slump Breccia Member. The latter unit is prominent and  
175 mappable, but in detail there are many thinner and more discontinuous breccias of this type  
176 (Moseley and Ford, 1985), including the Park Breccia, which is developed over a thickness of  
177 about 100 m. The term ‘Sliding Stone Slump Breccia Member’ is therefore used here to cover  
178 the whole of this interval (see Fig. 1). Stratigraphic equivalence of the Park Breccia and  
179 Sliding Stone Slump Breccia is important. A precise age for the Park Breccia therefore places

180 a good temporal constraint on the Ediacaran macrofossils preserved on the Mercian  
181 Assemblage bedding plane described in detail by Wilby et al. (2011). This bedding plane,  
182 with over 200 fossil impressions including the holotypes of *Bradgatia linfordensis* and  
183 *Charnia grandis* (Boynton and Ford, 1995) occurs only ca. 5 metres above the Sliding Stone  
184 Slump Breccia as seen in Bradgate Park.

185 The Park Breccia sample, JNC 912, was collected from a cutting on the A50 road  
186 (BNG SK 4860 1095) at the same locality as sample CH2 of Compston et al. (2002). It is a  
187 massive, medium-grained, volcaniclastic sandstone containing generally small cm-scale  
188 discrete mudstone rafts. In thin section, the matrix to these rafts is crammed with fine sand-  
189 size, angular to subrounded lithic volcanic grains. About 50% of these are composed of  
190 sparsely porphyritic andesite in which plagioclase laths and microlites show fluxional to  
191 decussate orientation; the remainder consist of andesite with non-oriented textures ranging  
192 from aphanitic through to microcrystalline and microgranular types. Between these grains are  
193 angular fragments of quartz and feldspar (DR Fig. 1d). The sedimentary clasts consist of  
194 volcaniclastic mudstone and siltstone. Like the Sliding Stone Slump Breccia, the Park  
195 Breccia is interpreted as being deposited from sediment gravity flows generated by submarine  
196 slumping of only partially lithified volcaniclastic material.

197 The Hanging Rocks Formation was analysed for its detrital zircon characteristics  
198 because it provides evidence of epiclastic sedimentation in the terminal part of the Charnian  
199 Supergroup. It also occupies an important and somewhat controversial stratigraphical  
200 position (Fig. 2) at the top of the Maplewell Group. Sample JNC 846 was collected from the  
201 type locality on Charnwood Forest Golf Course (BNG SK 5244 1502). It is a medium-  
202 grained poorly sorted micaceous sandstone, with abundant rounded granules and small  
203 pebbles and aligned slivers of siltstone (DR Fig. 1e). Thin sections show that many granules  
204 and pebbles have lithologies ‘exotic’ to those found in the underlying Charnian strata. These  
205 exotic grains include meta-quartzite with sutured grain boundaries and muscovite laths,

206 various polycrystalline quartz aggregates, and perthitic alkali feldspar. The majority of the  
207 other lithic grains are volcanic and include andesites and dacites with microcrystalline,  
208 microgranular, and in a few cases, intergranular textures. These resemble the lithic grains in  
209 the underlying Charnian formations. Other volcanic grains in the rock, however, do not and  
210 include various types of welded tuff with fluidal and shardic textures, some with marginally  
211 melted quartz xenocrysts (Carney, 1994; 2000c). The good to moderate rounding and  
212 sphericity of lithic grains and individual crystals in this formation is a further feature setting  
213 this unit apart from lithologies in the underlying formations (see also discussion on the  
214 geochemistry of the pebbles, below).

215

## 216 **U-Pb Results**

### 217 ***Blackbrook Group***

218 LA-ICP-MS results are summarised in DR Table 1. The dominant zircon population of JNC  
219 836 has a  $^{206}\text{Pb}/^{238}\text{U}$  age of  $611_{-4}^{+2}$  Ma (n=55, coherent group of 49) for <5% discordant  
220 zircons (as calculated with the TuffZirc age extraction algorithm; Ludwig, 2003; Ludwig and  
221 Mundil, 2002). Also present are xenocrystic grain cores with  $^{206}\text{Pb}/^{238}\text{U}$  ages of  $630 \pm 12$   
222 Ma,  $703 \pm 14$  Ma,  $1045 \pm 18$  Ma,  $1228 \pm 20$  Ma and  $1484 \pm 29$  Ma. The stratigraphically  
223 younger South Quarry Breccia sample, JNC 917, has a zircon population with a weighted  
224 mean  $^{206}\text{Pb}/^{238}\text{U}$  age of  $611 \pm 2$  Ma (TuffZirc, n = 76, coherent group of 68),  
225 indistinguishable from the age of the JNC 836 zircons.

226 A summary of the CA-ID-TIMS ages and the entire data set are presented in Tables 2  
227 and DR Table 2, respectively. Almost all of the data for JNC 916, 836 and 917 cluster on or  
228 near concordia between ca. 611 Ma and ca. 620 Ma. This mirrors the main cluster of LA-  
229 ICP-MS data for these three rocks. The CA-TIMS data for all three samples completely  
230 overlaps, as does the age of the youngest grain analysed from each stratigraphic horizon. For  
231 purposes of TIMS-ICP comparison, the pooled CA-TIMS data yield a TuffZirc  $^{206}\text{Pb}/^{238}\text{U}$

232 age of  $613.9^{+1.4}_{-0.5}$  Ma (n = 38). Separate from this main group are two data points with slightly  
233 older  $^{206}\text{U}/^{238}\text{U}$  ages of ca. 622 Ma.

234

235 ***Beacon Hill Formation (Maplewell Group)***

236 LA-ICP-MS analysis of JNC 918 reveals a zircon population differing from the underlying  
237 Blackbrook Group samples by virtue of the presence of a younger ca. 570 Ma component.  
238  $^{206}\text{Pb}/^{238}\text{U}$  ages of <5% discordant grains form an asymmetric distribution with a TuffZirc  
239  $^{206}\text{Pb}/^{238}\text{U}$  age of  $599^{+3}_{-5}$  Ma (n = 61, coherent group of 52). The Isoplot age population  
240 unmixing utility based on Sambridge and Compston (1994) yields two age components at  
241  $600 \pm 2$  Ma and  $569 \pm 7$  Ma.

242 CA-ID-TIMS data for JNC 918 includes analyses of <600 Ma grains identified by  
243 LA-ICP-MS that were extracted from the epoxy grain mount as well as additional unmounted  
244 grains. CA-TIMS confirms the presence of <600 Ma grains, and two analyses have  $^{206}\text{U}/^{238}\text{U}$   
245 ages of ca. 569 Ma. One further analysis is younger than the two overlapping concordant ca.  
246 569 Ma grains but is imprecise and concordant by virtue of its large uncertainties. It was  
247 included here to further illustrate the presence of <600 Ma zircons but is not used in the  
248 calculation of the age of this volcaniclastic rock because of its proportionally large common  
249 Pb correction and consequent diminished reliability. Also present are a main zircon  
250 population at 611-618 Ma that overlaps completely with the dominant zircon populations of  
251 the underlying Blackbrook Group rocks.

252 Carney and Noble (2007) reported CA-ID-TIMS data for JNC 911 that substantiates the ca.  
253 600 Ma and younger zircon ages yielded by JNC 918 from the Beacon Hill Formation. The  
254 JNC 911 data were obtained prior to the development of the EARTHTIME tracer and instead  
255 used the original T. Krogh  $^{205}\text{Pb}-^{235}\text{U}$  tracer that was prepared at the Department of  
256 Terrestrial Magnetism, Carnegie Institution, Washington D.C. in the 1970's. The calibration

257 of this older spike was checked using U-Pb gravimetric solutions at the Jack Satterley  
258 Geochronology Laboratory, Toronto. These same gravimetric solutions were in turn shown  
259 to be accurate compared to other more recently mixed U-Pb gravimetric solutions used to  
260 calibrate the EARTHTIME  $^{205}\text{Pb}$ - $^{233}\text{U}$ - $^{235}\text{U}$  tracer. Potential bias in data produced using  
261 either of the tracers is therefore not significant at the level of the quoted uncertainties for  
262 these legacy data. Of the four analyses obtained for JNC 911, two grains give a  $^{206}\text{Pb}/^{238}\text{U}$   
263 age of  $611.6 \pm 1.4$  Ma, while two younger discordant grains give  $^{206}\text{Pb}/^{238}\text{U}$  ages of  $582.5 \pm$   
264  $0.4$  and  $590.5 \pm 0.3$  Ma, either reflecting Pb-loss from ca. 600 Ma or probably more likely  
265 analysed mixtures of  $\geq 611$  Ma cores and younger rims not completely removed by air  
266 abrasion. Additional data produced during the present study using the EARTHTIME tracer  
267 revealed only  $>611$  Ma zircons.

268 Of the limited number of grains ( $n = 5$ ) analysed from JNC 907, CA-ID-TIMS data indicate  
269 an old ca. 613 Ma component and a younger ca. 567-565 Ma component. Two of the  
270 younger grains overlap within uncertainty ( $^{206}\text{Pb}/^{238}\text{U} = 565.2 \pm 0.3$  Ma) which are  
271 interpreted to be the age of this rock.

272

### 273 ***Bradgate Formation (Maplewell Group)***

274 For JNC 912, sampled from the Park Breccia at the base of the Bradgate Formation, CA-ID-  
275 TIMS analysis reveals two widely differing age groups. The oldest, represented by three  
276 concordant analyses, yields a  $^{206}\text{Pb}/^{238}\text{U}$  age of  $613.5 \pm 3.4$  Ma, consistent with the zircons  
277 dated from the underlying volcanic and volcaniclastic rocks. The younger zircons in the Park  
278 Breccia, also concordant, yield a  $^{206}\text{Pb}/^{238}\text{U}$  age of  $561.9 \pm 0.3$  Ma based on seven concordant  
279 analyses. The coherence of this group of analyses strongly indicates that this horizon was  
280 deposited during a single eruptive event. These new data generated with the EARTHTIME  
281 tracer are in agreement with previously reported legacy TIMS data ( $561.9 \pm 1.9$  Ma,  $n = 4$ ) on

282 similar zircon grains produced with the T. Krogh Carnegie  $^{205}\text{Pb}/^{235}\text{U}$  tracer (Carney and  
283 Noble, 2007, Wilby et al., 2011).

284

285 ***Hanging Rocks Formation (Maplewell Group)***

286 JNC 846 LA-ICP-MS detrital zircon ages concentrate in the range 750-560 Ma, with a very  
287 few Mesoproterozoic to Archaean grains ( $n = 78$ ). Pre-Neoproterozoic grains are dated at  
288  $1176 \pm 36$  Ma,  $2076 \pm 55$  Ma and  $2597 \pm 76$  Ma. Unmixing calculations on the  
289 Neoproterozoic data yield peaks at  $729 \pm 9$  Ma,  $673 \pm 19$  Ma,  $608 \pm 2$  Ma and  $562 \pm 6$  Ma.  
290 Focussing further on the youngest zircons ( $n = 4$ ), these have a mean  $^{206}\text{Pb}/^{238}\text{U}$  age of  $557 \pm$   
291 6 Ma, interpreted as dating (albeit imprecisely), the youngest material sampled within the  
292 Maplewell Group. CA-TIMS analysis of young grains extracted from the LA-ICP-MS grain  
293 mount was attempted but abandoned due to a mismatch in grain indexing. Further work on  
294 this formation will be pursued, but was beyond the scope of this study.

295

296 **Chemical compositions of Hanging Rocks Formation volcanic pebbles**

297 The conglomerates of this formation represent the first appearance of unequivocally  
298 epiclastic material in the Charnian Supergroup. Although the rounded pebbles and granules  
299 indicate an early history of reworking in shallow waters by wave or current agitation, the  
300 overall sedimentary architecture of the Hanging Rocks Formation suggests that final  
301 transport to the Charnian depo-basin was by the agency of turbidity currents (Carney, 2000c).  
302 Geochemical data from three volcanic pebbles separated from a conglomerate sample were  
303 investigated by two of us (TCP and JNC) to better characterize the sources of volcanogenic  
304 detritus available to the Charnwood region late in the development of the volcanic and  
305 sedimentary activity. Whole-rock chemical compositions for the pebbles are reported in DR  
306 Table 3, and their geochemistry indicates that the pebbles have major and trace element  
307 compositions akin to those of igneous rocks from the concealed ca. 600-620 Ma Fenland

308 Terrane (Noble et al., 1993; Pharaoh et al., 1991; Pharaoh and Carney, 2000). The latter are  
309 chemically more evolved than the Charnian Supergroup (e.g. higher SiO<sub>2</sub>, LILE's), and this  
310 relationship is reflected by HFSE trace element distributions for Zr and Y shown in DR Fig.  
311 5. On this diagram, the Hanging Rocks pebbles plot in a field outlined by igneous rocks of  
312 the Fenland Terrane, and are quite distinct from the more HFSE-depleted Charnwood  
313 igneous and volcanic rocks. Note that the crystal-rich Caldecote Formation volcaniclastic  
314 strata exposed at Nuneaton (Fig. 1, inset) have similar Zr-Y characteristics to these  
315 Charnwood rocks, supporting their position within the Charnwood Terrane.

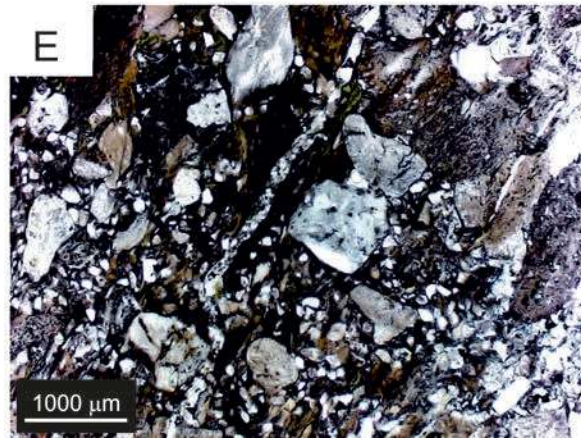
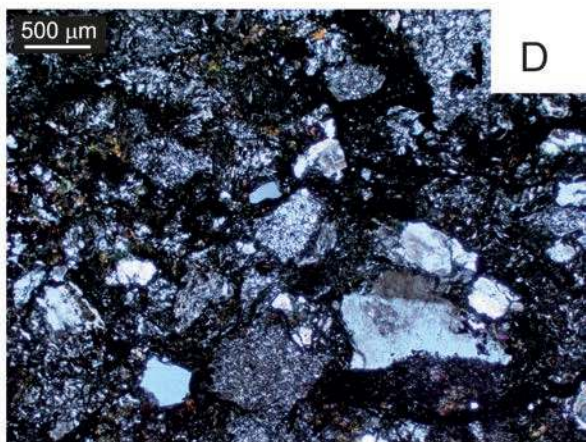
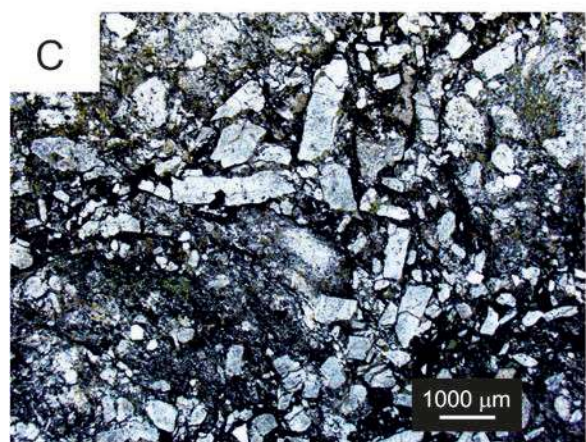
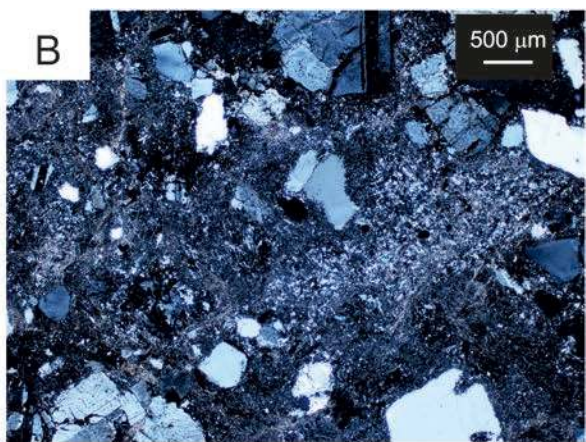
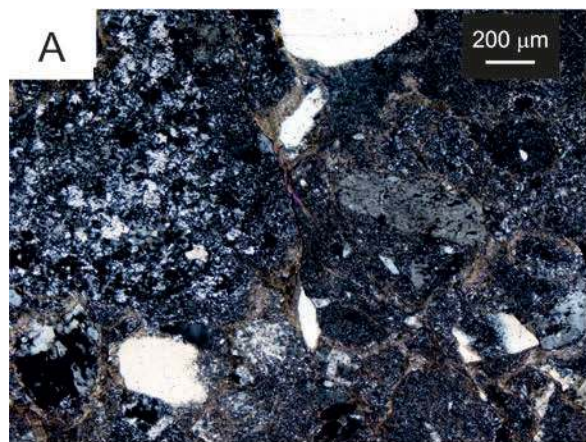
316

317 We conclude from this that the volcanic pebbles in the Hanging Rocks Formation most likely  
318 reflect a significant episode of uplift, emergence and fluvial and/or shoreline reworking  
319 within the Fenland Terrane, which lay adjacent to the Charnwood Terrane (Fig. 1, inset). For  
320 reference, geochemical data from Warren House Formation and Uriconian Group volcanic  
321 rocks of the Wrekin Terrane are also plotted in DR figure 5. These rocks are contemporaries  
322 of the Maplewell Group, with U-Pb ages in the range 565-560 Ma and (Tucker and Pharaoh,  
323 1991), and although the Uriconian samples compare geochemically with those from the  
324 Fenland Terrane/Hanging Rocks Formation cluster on DR Fig. 5, the Wrekin Terrane lies at a  
325 considerably greater distance from Charnwood than does the Fenland Terrane, and is thus  
326 less likely to be a source of the pebbles. Moreover, the Wrekin Terrane as a whole does not  
327 contain the c. 620-600 Ma zircon population that is characteristic of the Fenland Terrane and  
328 Hanging Rocks Formation. We note that the Padarn Tuff from the Cymru Terrane of north  
329 Wales has yielded U-Pb TIMS ages of c. 616 Ma (Tucker and Pharaoh, 1991) and SHRIMP  
330 ages of c. 605 Ma (Compston et al. 2002) and so, in terms of age at least, it represents an  
331 alternative potential source for the Hanging Rocks pebbles, albeit much more distal than the  
332 Fenland Terrane.

333

334 **Figure DR 1: Volcaniclastic rock textures**

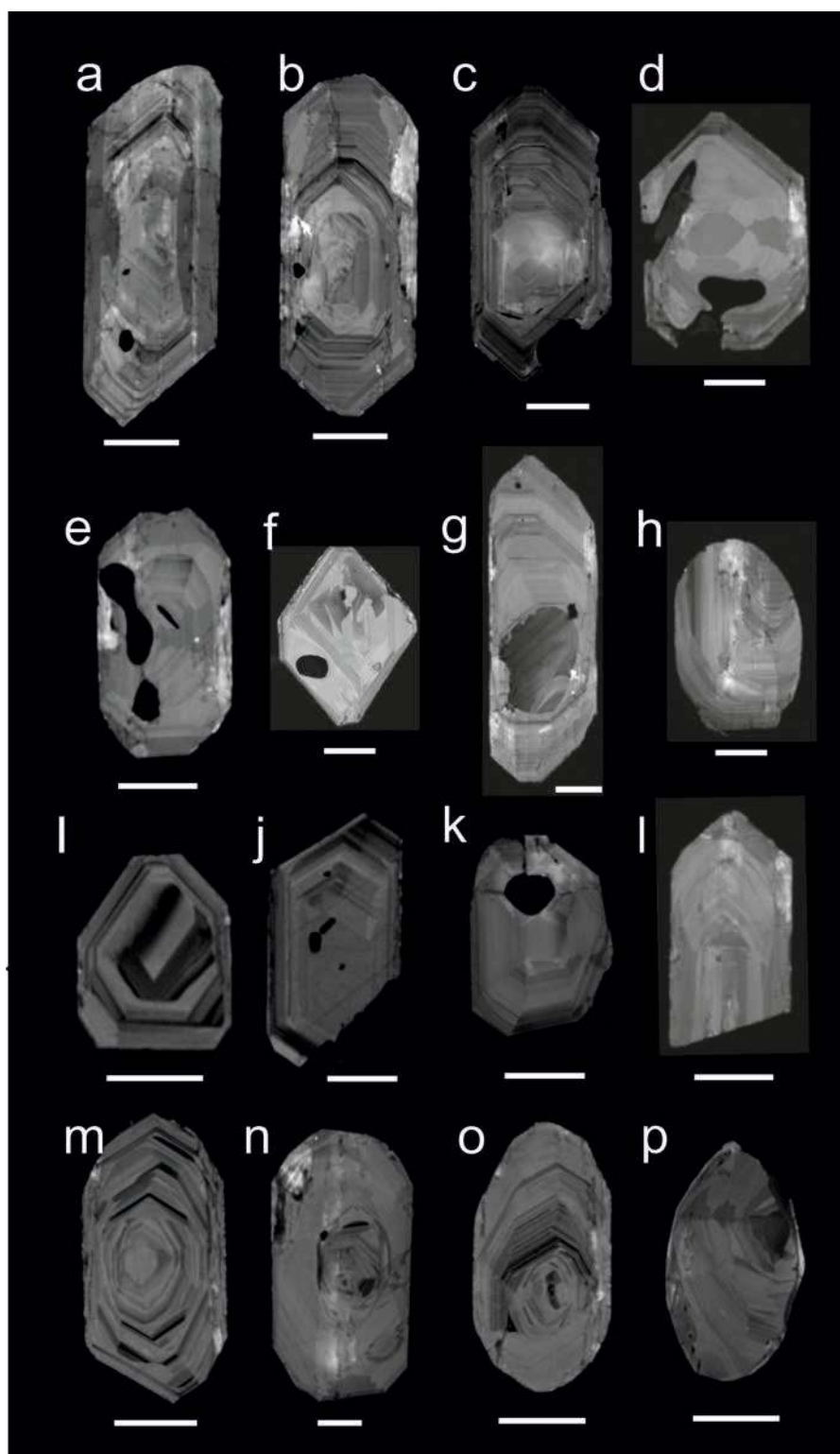
335 A. JNC 836 volcaniclastic sandstone Ives Head Formation (XPL). Close-packed  
336 andesite/dacite grains with microgranular and microcrystalline textures; quartz grains (white)  
337 show highly angular outlines (lower right) and magmatic rounding (crystal at top image). B.  
338 JNC 917 South Quarry Breccia volcaniclastic matrix (XPL). Centre of image shows close-  
339 packed microcrystalline andesite/dacite grains. Individual plagioclase crystals have angular  
340 outlines and subgrain development; quartz crystals (white areas) are angular with one grain  
341 (lower right) interpreted as a magmatically abraded euhedra with marginal gas bubble  
342 incursion. C. JNC 918 Benscliffe Breccia crystal-enriched matrix (PPL). ‘Trains’ of close-  
343 packed plagioclase and quartz crystals separate andesitic and dacitic lapilli. Crystals are  
344 euhedral to sharply angular, with no evidence of abrasion other than that which can be  
345 ascribed to collisions during mass-transport. D. JNC 912 Park Breccia volcaniclastic  
346 sandstone matrix (XPL). Angular plagioclase and quartz crystals, abundant angular to  
347 subangular andesite and dacite grains; textures of latter show variation between  
348 microcrystalline and finely microgranular, with fluxional texture visible in the grain at top-  
349 right. E. JNC 846 Hanging Rocks Formation sandstone (PPL). Sandstone is poorly sorted,  
350 with silt-size to medium sand-size andesite and dacite grains; elliptical clast shows tectonic  
351 foliation (top-centre of image). Larger well-rounded grains are embedded in silt- to mud-rich  
352 matrix.



353

354

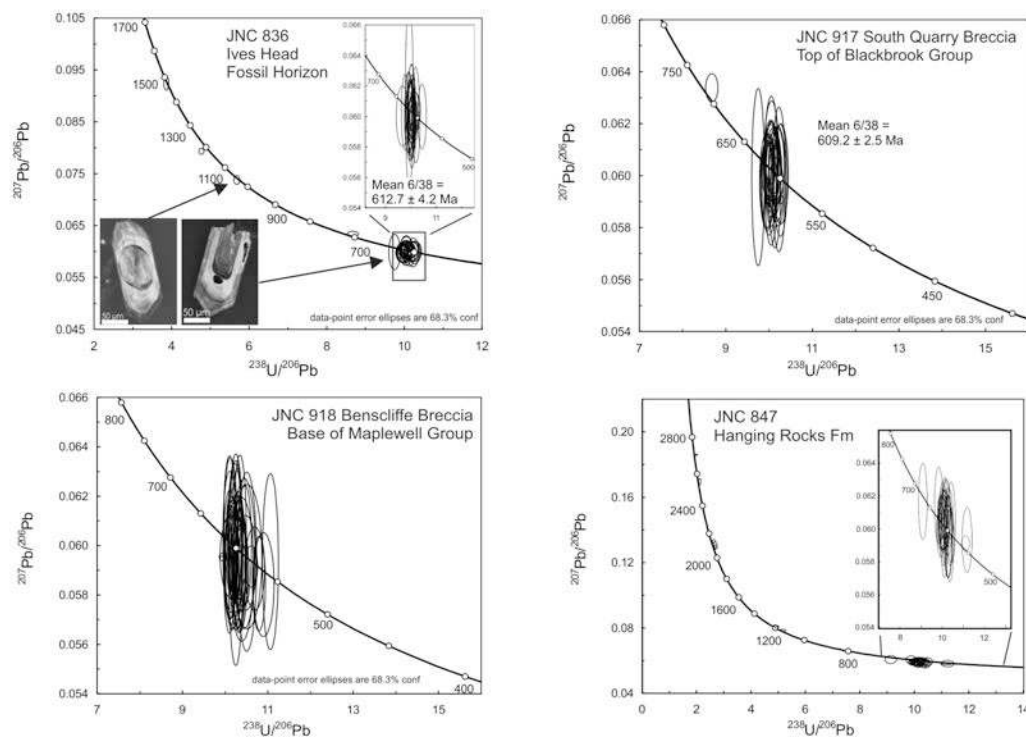
355 **Figure DR 2. SEM-CL images for typical Charnwood zircons.** A-F: Euhedral zircons  
356 typical of the Blackbrook Group rocks, showing melt/mineral inclusions and typical zoning.  
357 G: Euhedral zircon with prominent xenocrystic core. H: Rare rounded zircon.  
358 I-N: Euhedral zircons typical of all the Maplewell Group rocks. O-P: Rounded detrital  
359 zircons specifically from the Hanging Rocks Formation, Maplewell Group. Scale bars are 25  
360  $\mu\text{m}$ .



361

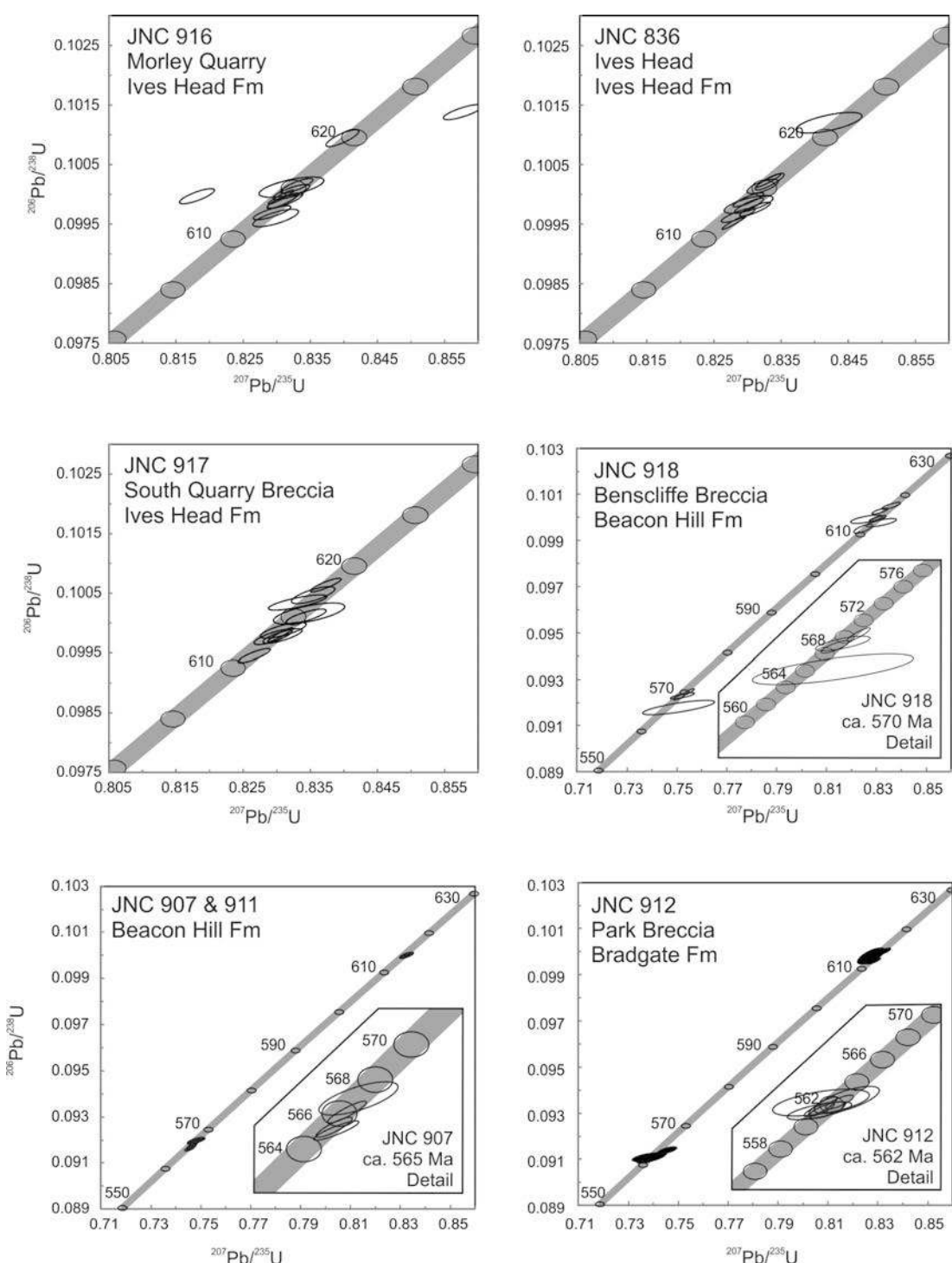
362 **Figure DR 3. Tera-Wasserburg diagrams for LA-ICPMS zircon U-Pb data.** Data are  
363 plotted at the  $\pm 1\sigma$  level, and are the <5% discordant grains in Table DR2. Insets illustrate c.  
364 600 Ma data in detail.

365  
366  
367



368  
369

370 **Figure DR 4. Concordia diagrams for CA-TIMS zircon U-Pb data.** Data are plotted at  
 371 the  $\pm 2\sigma$  level. Insets illustrate data used to calculate deposition ages.  
 372



373

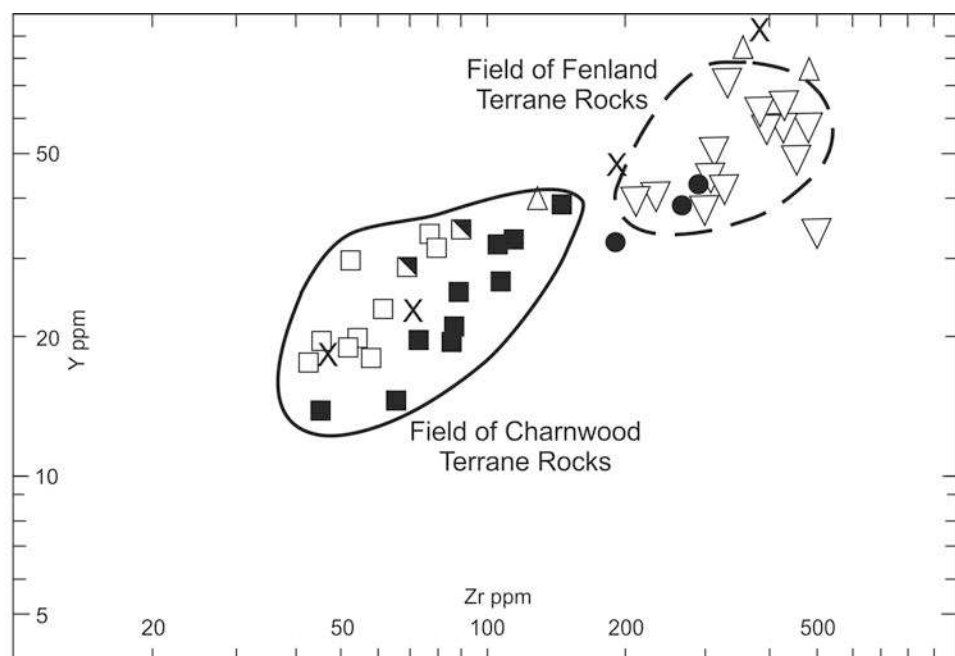
374

375

376 **Figure DR 5. Midlands Microcraton Zr and Y characteristics.** Data sources are (1) DR  
 377 Table 3 ; (2) Pharaoh et al., (1987; primary igneous rocks); Carney (2000); (3) Pharaoh and  
 378 Evans (1987); (4) Bridge et al. (1998); (5) Pharaoh et al. (1991), and (6) Bevins et al. (1995).

379

380



## Charnwood Terrane

- Volcanic pebbles in Hanging Rocks Formation<sup>1</sup>
- Maplewell Group, igneous rocks<sup>3</sup>
- Blackbrook Group, igneous rocks<sup>3</sup>
- Caldecote Volcanic Formation tuffs<sup>4</sup>

Charnwood Forest

Nuneaton

## Fenland Terrane

- ▽ Volcanic lithologies in Orton, Glinton and Oxendon Hall boreholes<sup>5</sup>

## Wrekin Terrane

- △ Uriconian Volcanic Group, Wrekin<sup>3</sup>
- ✗ Warren House Group, Malverns<sup>3</sup>

381

**Table DR 1.** U-Pb LA-ICP-MS U-Pb isotope data ( $\leq 10\%$  discordant).

Sample and grain	Ion Beam Intensities (mV)			Concentrations		Isotope Ratios (not corrected for common Pb)						Age (Ma)				
	$^{206}\text{Pb}$	$^{207}\text{Pb}$	$^{238}\text{U}$	U (ppm)	Pb (ppm)	$\frac{^{238}\text{U}}{^{206}\text{Pb}}$	$\pm 1\sigma \%$ err	$\frac{^{207}\text{Pb}}{^{206}\text{Pb}}$	$\pm 1\sigma \%$ err	$\frac{^{207}\text{Pb}}{^{235}\text{U}}$	$\pm 1\sigma \%$ err	$\frac{^{206}\text{Pb}}{^{238}\text{U}}$	$\pm 1\sigma \%$ err	corr. coef.	$\frac{^{206}\text{Pb}}{^{238}\text{U}}$	$\pm 2\sigma$ abs
<b>JNC 836 (BNG SK 4772 1700), Blackbrook Group, Ives Head Fm at Ives Head, turbidite bed, volcaniclastic sandstone</b>																
1	0.7	0.04	10	109	11	9.89	0.99	0.0589	2.18	0.821	2.40	0.1011	0.99	0.41	621	12
2	1.0	0.05	15	152	16	9.88	1.08	0.0590	1.63	0.824	1.96	0.1012	1.08	0.55	621	13
4	0.8	0.04	12	125	12	9.98	0.99	0.0588	1.99	0.813	2.22	0.1002	0.99	0.45	616	12
5	0.4	0.03	6	65	7	9.84	1.16	0.0628	3.21	0.880	3.41	0.1016	1.16	0.34	624	14
6	0.8	0.05	13	132	13	9.92	1.19	0.0591	1.84	0.821	2.19	0.1008	1.19	0.54	619	14
7	0.6	0.04	10	105	10	10.13	1.10	0.0591	2.30	0.805	2.55	0.0987	1.10	0.43	607	13
10 (rim)	0.7	0.04	11	116	12	10.10	1.10	0.0587	2.14	0.801	2.40	0.0990	1.10	0.46	609	13
11	0.7	0.04	11	116	11	10.13	1.04	0.0591	2.13	0.804	2.37	0.0987	1.04	0.44	607	12
12	1.1	0.10	7	69	18	3.86	1.11	0.0925	0.97	3.300	1.48	0.2589	1.11	0.75	1484	29
13	0.7	0.04	11	112	11	10.00	1.08	0.0597	2.15	0.823	2.41	0.1000	1.08	0.45	614	13
14	1.0	0.05	15	159	16	10.13	0.93	0.0588	1.59	0.800	1.85	0.0987	0.93	0.51	607	11
16	0.7	0.04	11	114	11	10.03	0.97	0.0591	2.12	0.812	2.33	0.0997	0.97	0.42	613	11
18	0.9	0.05	14	144	14	10.04	1.09	0.0604	1.73	0.830	2.05	0.0996	1.09	0.53	612	13
19	0.9	0.05	14	142	14	10.10	1.20	0.0603	1.75	0.823	2.12	0.0990	1.20	0.57	609	14
20 - core	4.6	0.35	34	353	73	4.82	0.99	0.0838	0.32	2.398	1.04	0.2075	0.99	0.95	1215	22
20 - rim	0.6	0.03	10	102	10	10.26	0.99	0.0598	2.39	0.804	2.59	0.0975	0.99	0.38	599	11
21	0.6	0.03	9	92	9	10.13	0.92	0.0596	2.59	0.811	2.75	0.0987	0.92	0.33	607	11
22	0.6	0.03	9	96	10	9.95	1.12	0.0587	2.51	0.814	2.75	0.1005	1.12	0.41	618	13
23	0.9	0.05	13	135	14	9.64	1.00	0.0587	1.79	0.839	2.05	0.1038	1.00	0.49	636	12
24	0.8	0.04	12	128	13	10.06	1.03	0.0603	1.90	0.827	2.16	0.0994	1.03	0.48	611	12
25	0.7	0.04	11	115	12	9.89	1.02	0.0585	2.12	0.816	2.35	0.1011	1.02	0.43	621	12
26	0.7	0.04	10	108	11	9.81	1.02	0.0583	2.23	0.819	2.45	0.1019	1.02	0.42	626	12
28	1.2	0.07	19	194	19	10.02	0.97	0.0588	1.35	0.809	1.66	0.0998	0.97	0.58	613	11
31	1.8	0.13	16	167	29	5.68	0.93	0.0738	0.78	1.791	1.21	0.1760	0.93	0.77	1045	18
32	0.4	0.02	6	58	6	9.75	1.01	0.0599	3.76	0.848	3.90	0.1026	1.01	0.26	630	12
33	1.0	0.06	16	168	17	10.04	1.04	0.0592	1.55	0.813	1.87	0.0996	1.04	0.56	612	12
34	0.8	0.04	12	123	12	10.10	0.94	0.0591	2.01	0.807	2.22	0.0990	0.94	0.42	609	11
35	0.8	0.05	13	131	13	9.76	0.88	0.0594	1.84	0.840	2.04	0.1025	0.88	0.43	629	11
36	0.6	0.03	9	91	9	9.88	1.11	0.0584	2.55	0.816	2.78	0.1012	1.11	0.40	622	13

Sample and grain	Ion Beam Intensities (mV)			Concentrations		Isotope Ratios (not corrected for common Pb)									Age (Ma)	
	$^{206}\text{Pb}$	$^{207}\text{Pb}$	$^{238}\text{U}$	U (ppm)	Pb (ppm)	$\frac{^{238}\text{U}}{^{206}\text{Pb}}$	$\pm 1\sigma$ % err	$\frac{^{207}\text{Pb}}{^{206}\text{Pb}}$	$\pm 1\sigma$ % err	$\frac{^{207}\text{Pb}}{^{235}\text{U}}$	$\pm 1\sigma$ % err	$\frac{^{206}\text{Pb}}{^{238}\text{U}}$	$\pm 1\sigma$ % err	corr. coef.	$\frac{^{206}\text{Pb}}{^{238}\text{U}}$	$\pm 2\sigma$ abs
<b>JNC 836 (BNG SK 4772 1700), Blackbrook Group, Ives Head Fm at Ives Head, turbidite bed, volcaniclastic sandstone.</b>																
37	3.1	0.23	23	239	50	4.77	0.91	0.0793	0.51	2.295	1.04	0.2098	0.91	0.87	1228	20
38	0.5	0.03	7	75	7	10.18	1.03	0.0590	3.16	0.799	3.32	0.0983	1.03	0.31	604	12
39	1.0	0.06	16	166	16	10.04	1.06	0.0587	1.57	0.806	1.89	0.0996	1.06	0.56	612	12
40	0.7	0.04	11	116	11	10.27	1.13	0.0601	2.12	0.807	2.40	0.0974	1.13	0.47	599	13
41	0.5	0.03	8	87	8	10.26	1.12	0.0612	2.72	0.823	2.95	0.0974	1.12	0.38	599	13
42	0.6	0.03	9	90	9	10.04	0.96	0.0597	2.64	0.820	2.81	0.0996	0.96	0.34	612	11
43	0.5	0.03	7	77	7	10.23	1.00	0.0599	3.08	0.807	3.23	0.0978	1.00	0.31	601	11
44	0.7	0.04	11	115	11	10.21	1.07	0.0600	2.11	0.810	2.37	0.0980	1.07	0.45	603	12
46	0.5	0.03	8	85	8	10.05	1.02	0.0605	2.73	0.831	2.92	0.0995	1.02	0.35	612	12
47	0.6	0.03	9	98	10	10.06	1.12	0.0606	2.44	0.831	2.69	0.0994	1.12	0.42	611	13
48	1.4	0.08	22	229	23	10.10	1.27	0.0603	1.13	0.824	1.70	0.0990	1.27	0.75	609	15
49	1.0	0.05	15	157	15	10.17	1.19	0.0604	1.61	0.819	2.00	0.0983	1.19	0.59	605	14
50	0.8	0.04	12	128	13	9.96	0.99	0.0596	1.92	0.825	2.16	0.1004	0.99	0.46	617	12
51	0.9	0.05	13	134	14	9.94	1.04	0.0596	1.83	0.827	2.11	0.1006	1.04	0.49	618	12
52	1.2	0.07	19	198	19	10.04	0.97	0.0609	1.34	0.837	1.65	0.0996	0.97	0.59	612	11
53	1.2	0.07	19	195	19	9.98	0.98	0.0603	1.31	0.833	1.63	0.1002	0.98	0.60	615	11
54	0.8	0.04	10	113	11	9.79	0.93	0.0584	2.04	0.822	2.24	0.1021	0.93	0.41	627	11
55	0.8	0.04	11	115	11	9.90	0.94	0.0588	2.04	0.819	2.24	0.1010	0.94	0.42	620	11
57	3.0	0.18	36	394	41	8.67	1.08	0.0634	0.57	1.007	1.22	0.1153	1.08	0.88	703	14
58	1.3	0.07	17	189	17	10.01	0.98	0.0593	1.30	0.816	1.63	0.0999	0.98	0.60	614	11
59	0.8	0.04	10	111	10	9.95	1.09	0.0598	2.02	0.829	2.30	0.1005	1.09	0.47	618	13
60	1.1	0.06	15	163	15	10.10	1.07	0.0603	1.45	0.823	1.80	0.0990	1.07	0.59	609	12
61	1.2	0.07	17	181	16	10.17	1.02	0.0595	1.36	0.806	1.70	0.0983	1.02	0.60	604	12
62	1.1	0.06	16	169	15	10.12	0.98	0.0598	1.41	0.814	1.72	0.0988	0.98	0.57	607	11
63	0.7	0.04	9	102	9	10.22	0.98	0.0586	2.25	0.791	2.46	0.0978	0.98	0.40	602	11
64	0.8	0.04	11	115	10	10.24	0.92	0.0591	2.03	0.795	2.23	0.0977	0.92	0.41	601	11
65	0.5	0.03	7	77	7	10.12	0.96	0.0589	2.88	0.802	3.03	0.0988	0.96	0.32	607	11
66	1.2	0.06	16	176	16	10.15	0.95	0.0590	1.39	0.801	1.69	0.0986	0.95	0.56	606	11
67	0.8	0.04	11	119	11	10.14	0.95	0.0580	2.02	0.788	2.23	0.0986	0.95	0.42	606	11

Sample and grain	Ion Beam Intensities (mV)			Concentrations		Isotope Ratios (not corrected for common Pb)									Age (Ma)	
	$^{206}\text{Pb}$	$^{207}\text{Pb}$	$^{238}\text{U}$	U (ppm)	Pb (ppm)	$\frac{^{238}\text{U}}{^{206}\text{Pb}}$	$\pm 1\sigma$ % err	$\frac{^{207}\text{Pb}}{^{206}\text{Pb}}$	$\pm 1\sigma$ % err	$\frac{^{207}\text{Pb}}{^{235}\text{U}}$	$\pm 1\sigma$ % err	$\frac{^{206}\text{Pb}}{^{238}\text{U}}$	$\pm 1\sigma$ % err	corr. coef.	$\frac{^{206}\text{Pb}}{^{238}\text{U}}$	$\pm 2\sigma$ abs
<b>JNC 917 (BNG SK 4637 1712) Blackbrook Group, Ives Head Fm, South Quarry Breccia, volcaniclastic sandstone and mudstone breccia.</b>																
1	0.7	0.04	10	128	12	9.67	1.68	0.0600	2.18	0.856	2.75	0.1034	1.68	0.61	635	20
2	0.9	0.05	13	173	16	10.24	1.33	0.0589	1.80	0.792	2.24	0.0976	1.33	0.60	601	15
3-1	0.7	0.04	11	143	13	10.31	1.11	0.0589	2.22	0.788	2.49	0.0970	1.11	0.45	597	13
3-3	0.4	0.02	6	85	8	9.87	1.27	0.0590	3.28	0.824	3.52	0.1014	1.27	0.36	622	15
4	0.3	0.02	5	62	6	10.04	1.02	0.0589	4.35	0.810	4.47	0.0996	1.02	0.23	612	12
5	0.5	0.03	8	104	10	9.96	1.13	0.0596	2.73	0.824	2.95	0.1004	1.13	0.38	617	13
6	0.4	0.03	6	81	8	9.76	1.00	0.0735	4.33	1.039	4.44	0.1025	1.00	0.23	629	12
7	0.4	0.03	7	87	8	9.76	0.98	0.0639	2.98	0.903	3.14	0.1024	0.98	0.31	629	12
8	0.6	0.03	9	115	11	9.78	0.95	0.0589	2.48	0.830	2.65	0.1022	0.95	0.36	627	11
9-1	0.4	0.02	6	85	8	9.78	1.04	0.0576	3.27	0.812	3.43	0.1023	1.04	0.30	628	12
9-2	0.7	0.04	11	143	13	9.80	0.99	0.0597	2.04	0.840	2.27	0.1020	0.99	0.44	626	12
10	0.9	0.05	14	180	17	9.89	1.01	0.0596	1.69	0.831	1.97	0.1011	1.01	0.51	621	12
11	0.4	0.02	6	78	7	9.98	1.00	0.0593	3.58	0.819	3.72	0.1002	1.00	0.27	616	12
12	0.6	0.03	9	119	11	9.97	0.93	0.0601	2.40	0.830	2.58	0.1003	0.93	0.36	616	11
13	0.5	0.03	7	96	9	10.04	0.93	0.0592	2.99	0.814	3.13	0.0996	0.93	0.30	612	11
14	0.5	0.03	7	99	9	10.01	1.07	0.0573	2.97	0.789	3.16	0.0999	1.07	0.34	614	13
15	0.3	0.02	4	57	5	9.90	1.54	0.0874	8.74	1.217	8.88	0.1010	1.54	0.17	620	18
16	0.4	0.02	6	74	7	10.15	1.04	0.0564	3.83	0.766	3.97	0.0986	1.04	0.26	606	12
17	0.7	0.04	10	134	12	9.93	1.24	0.0596	2.21	0.828	2.54	0.1007	1.24	0.49	618	15
18-1	0.6	0.03	9	124	11	10.17	1.33	0.0590	2.43	0.800	2.77	0.0983	1.33	0.48	604	15
18-2	0.5	0.03	8	105	9	10.15	1.21	0.0591	2.85	0.803	3.10	0.0985	1.21	0.39	606	14
19	0.3	0.02	5	61	6	10.09	1.14	0.0586	4.44	0.801	4.58	0.0991	1.14	0.25	609	13
20-1	0.3	0.02	5	61	6	10.09	1.14	0.0586	4.44	0.801	4.58	0.0991	1.14	0.25	609	13
20-1	0.5	0.03	8	109	10	10.29	1.08	0.0610	2.76	0.818	2.97	0.0972	1.08	0.36	598	12
21	0.6	0.04	9	126	12	10.06	1.56	0.0586	2.31	0.803	2.79	0.0994	1.56	0.56	611	18
22	1.2	0.07	19	251	23	10.15	1.49	0.0604	1.28	0.820	1.96	0.0985	1.49	0.76	606	17
23	0.9	0.06	14	192	17	10.29	1.42	0.0652	2.01	0.873	2.46	0.0972	1.42	0.58	598	16
24	1.2	0.07	19	247	22	10.07	0.89	0.0597	1.32	0.817	1.59	0.0993	0.89	0.56	610	10
25-1	0.7	0.04	10	139	13	10.01	1.04	0.0594	2.12	0.818	2.36	0.0999	1.04	0.44	614	12

Sample and grain	Ion Beam Intensities (mV)			Concentrations		Isotope Ratios (not corrected for common Pb)									Age (Ma)	
	$^{206}\text{Pb}$	$^{207}\text{Pb}$	$^{238}\text{U}$	U (ppm)	Pb (ppm)	$\frac{^{238}\text{U}}{^{206}\text{Pb}}$	$\pm 1\sigma$ % err	$\frac{^{207}\text{Pb}}{^{206}\text{Pb}}$	$\pm 1\sigma$ % err	$\frac{^{207}\text{Pb}}{^{235}\text{U}}$	$\pm 1\sigma$ % err	$\frac{^{206}\text{Pb}}{^{238}\text{U}}$	$\pm 1\sigma$ % err	corr. coef.	$\frac{^{206}\text{Pb}}{^{238}\text{U}}$	$\pm 2\sigma$ abs
	<b>JNC 917 (BNG SK 4637 1712) Blackbrook Group, Ives Head Fm, South Quarry Breccia, volcaniclastic sandstone and mudstone breccia.</b>															
25-2	0.9	0.05	14	184	17	10.02	0.88	0.0598	1.68	0.823	1.90	0.0998	0.88	0.46	613	10
26	0.5	0.03	8	100	9	9.97	0.99	0.0614	2.86	0.849	3.02	0.1003	0.99	0.33	616	12
27	0.5	0.03	8	104	9	10.01	0.97	0.0599	2.75	0.826	2.92	0.0999	0.97	0.33	614	11
28	0.8	0.04	11	151	14	10.04	0.96	0.0609	1.96	0.836	2.18	0.0996	0.96	0.44	612	11
29-1	0.4	0.02	6	84	7	10.19	1.00	0.0611	3.29	0.827	3.44	0.0981	1.00	0.29	603	12
29-2	0.4	0.02	6	76	7	10.05	1.05	0.0629	3.39	0.863	3.55	0.0995	1.05	0.30	612	12
30	0.5	0.03	8	106	10	10.06	1.00	0.0621	2.60	0.851	2.78	0.0994	1.00	0.36	611	12
31-1	0.5	0.03	8	104	10	10.05	1.13	0.0693	3.20	0.951	3.39	0.0995	1.13	0.33	612	13
31-2	0.7	0.04	11	145	13	10.25	1.29	0.0617	2.05	0.830	2.42	0.0975	1.29	0.53	600	15
33-1	0.6	0.04	10	130	12	10.09	0.94	0.0627	2.18	0.857	2.38	0.0991	0.94	0.40	609	11
33-2	0.4	0.03	6	86	8	10.55	1.26	0.0670	3.18	0.876	3.42	0.0948	1.26	0.37	584	14
34	0.4	0.02	6	75	7	10.14	1.15	0.0628	3.60	0.854	3.78	0.0986	1.15	0.30	606	13
35-1	0.5	0.03	8	107	10	9.98	1.12	0.0591	2.69	0.816	2.92	0.1002	1.12	0.38	616	13
35-2	0.5	0.03	7	96	9	9.92	1.09	0.0602	2.93	0.837	3.12	0.1008	1.09	0.35	619	13
36	0.6	0.05	9	124	11	9.75	1.09	0.0816	2.34	1.154	2.59	0.1026	1.09	0.42	629	13
37	1.3	0.08	21	274	24	10.25	1.41	0.0621	1.20	0.836	1.86	0.0975	1.41	0.76	600	16
38	0.5	0.03	7	91	8	10.16	1.21	0.0622	2.97	0.844	3.20	0.0985	1.21	0.38	605	14
40	0.4	0.03	7	88	8	10.20	1.03	0.0630	3.08	0.851	3.25	0.0981	1.03	0.32	603	12
41	0.5	0.03	7	94	8	10.17	0.96	0.0617	2.97	0.837	3.13	0.0983	0.96	0.31	605	11
42	0.6	0.03	9	114	10	10.20	0.97	0.0625	2.48	0.845	2.66	0.0981	0.97	0.37	603	11
43	0.7	0.04	11	144	13	10.11	0.91	0.0620	2.01	0.845	2.20	0.0990	0.91	0.41	608	11
44	0.4	0.02	6	85	7	10.26	1.13	0.0624	3.19	0.839	3.39	0.0975	1.13	0.34	600	13
45	0.4	0.03	6	81	7	10.21	1.09	0.0824	3.08	1.113	3.27	0.0980	1.09	0.33	602	12
46-1	0.3	0.02	4	54	5	9.16	1.47	0.0724	4.31	1.090	4.56	0.1091	1.47	0.32	668	19
46-2	0.3	0.02	5	60	5	10.08	1.12	0.0641	4.26	0.877	4.41	0.0992	1.12	0.25	610	13
48-1	0.7	0.04	10	137	13	9.94	0.96	0.0604	2.14	0.838	2.35	0.1006	0.96	0.41	618	11
48-2	0.6	0.04	10	126	12	9.91	0.93	0.0608	2.28	0.846	2.46	0.1009	0.93	0.38	620	11
49	0.3	0.02	5	66	6	9.89	1.02	0.0594	4.06	0.829	4.19	0.1011	1.02	0.24	621	12
50	0.5	0.03	8	106	10	9.77	0.96	0.0603	2.72	0.851	2.89	0.1024	0.96	0.33	628	12
51-1	0.4	0.02	6	83	7	10.02	0.99	0.0604	3.37	0.830	3.52	0.0998	0.99	0.28	613	12

Sample and grain	Ion Beam Intensities (mV)			Concentrations		Isotope Ratios (not corrected for common Pb)									Age (Ma)	
	$^{206}\text{Pb}$	$^{207}\text{Pb}$	$^{238}\text{U}$	U (ppm)	Pb (ppm)	$\frac{^{238}\text{U}}{^{206}\text{Pb}}$	$\pm 1\sigma$ % err	$\frac{^{207}\text{Pb}}{^{206}\text{Pb}}$	$\pm 1\sigma$ % err	$\frac{^{207}\text{Pb}}{^{235}\text{U}}$	$\pm 1\sigma$ % err	$\frac{^{206}\text{Pb}}{^{238}\text{U}}$	$\pm 1\sigma$ % err	corr. coef.	$\frac{^{206}\text{Pb}}{^{238}\text{U}}$	$\pm 2\sigma$ abs
<b>JNC 917 (BNG SK 4637 1712) Blackbrook Group, Ives Head Fm, South Quarry Breccia, volcaniclastic sandstone and mudstone breccia.</b>																
51-2	0.4	0.02	6	83	8	9.86	0.92	0.0594	3.41	0.830	3.54	0.1014	0.92	0.26	622	11
52	1.2	0.07	19	252	22	10.13	1.05	0.0599	1.30	0.816	1.68	0.0987	1.05	0.63	607	12
53	0.3	0.02	5	67	6	10.13	1.02	0.0588	4.25	0.801	4.37	0.0988	1.02	0.23	607	12
54	0.6	0.03	9	116	10	10.20	1.03	0.0593	2.57	0.801	2.77	0.0981	1.03	0.37	603	12
55	0.7	0.05	11	149	14	9.90	1.10	0.0673	2.52	0.937	2.75	0.1010	1.10	0.40	620	13
56	1.1	0.06	18	241	21	10.07	1.24	0.0598	1.42	0.819	1.88	0.0993	1.24	0.66	610	14
57	0.3	0.02	5	68	6	10.06	1.15	0.0573	4.20	0.785	4.36	0.0994	1.15	0.26	611	13
58-1	1.3	0.07	19	257	23	10.07	1.01	0.0602	1.28	0.824	1.63	0.0993	1.01	0.62	610	12
58-2	0.5	0.03	8	107	9	10.04	0.97	0.0591	2.78	0.812	2.95	0.0996	0.97	0.33	612	11
59	0.6	0.04	10	127	11	10.03	1.03	0.0602	2.32	0.828	2.53	0.0997	1.03	0.41	613	12
60	0.6	0.04	10	133	12	10.44	1.08	0.0600	2.34	0.792	2.58	0.0958	1.08	0.42	590	12
61-1	0.5	0.03	7	96	9	10.00	1.11	0.0692	3.78	0.954	3.94	0.1000	1.11	0.28	614	13
61-2	0.4	0.02	6	74	7	10.05	1.14	0.0617	3.73	0.846	3.90	0.0995	1.14	0.29	611	13
62	0.5	0.03	8	101	9	10.01	1.03	0.0597	2.83	0.822	3.01	0.0999	1.03	0.34	614	12
63	0.8	0.05	13	170	15	10.02	1.15	0.0653	1.66	0.898	2.02	0.0998	1.15	0.57	613	13
64	0.6	0.03	9	115	10	10.18	1.01	0.0608	2.59	0.824	2.78	0.0983	1.01	0.36	604	12
66	0.3	0.02	5	64	6	10.07	1.17	0.0620	4.12	0.849	4.28	0.0993	1.17	0.27	611	14

**JNC 918 (BNG SK 5146 1246) Maplewell Group, Beacon Hill Fm, Benscliffe Breccia at Pillar Rock, Massive andesite breccia and coarse grained volcaniclastic sandstone.**

1	1.9	0.11	30	110	9	10.90	1.51	0.0584	2.37	0.739	2.81	0.0918	1.51	0.54	566	16
2	1.9	0.11	30	86	8	10.11	1.77	0.0619	2.67	0.845	3.20	0.0990	1.77	0.55	608	21
3	0.8	0.05	7	110	9	11.08	1.99	0.0578	2.45	0.720	3.16	0.0903	1.99	0.63	557	21
4	0.8	0.06	7	85	8	10.10	1.69	0.0587	2.77	0.801	3.25	0.0990	1.69	0.52	609	20
5	3.5	0.17	100	123	11	10.19	1.98	0.0596	1.97	0.806	2.80	0.0981	1.98	0.71	603	23
6	3.0	0.15	86	78	7	10.26	1.78	0.0582	3.07	0.782	3.55	0.0974	1.78	0.50	599	20
8	2.0	0.11	30	81	7	10.24	1.62	0.0592	2.89	0.797	3.31	0.0976	1.62	0.49	601	19
9	1.9	0.11	30	93	8	10.54	1.66	0.0605	2.51	0.791	3.01	0.0949	1.66	0.55	584	18
12	0.9	0.06	8	71	6	10.52	2.18	0.0596	3.24	0.781	3.90	0.0951	2.18	0.56	586	24
13	0.9	0.06	8	72	6	10.39	1.79	0.0590	3.25	0.784	3.71	0.0963	1.79	0.48	592	20
15	3.3	0.16	96	140	12	10.69	1.44	0.0591	1.88	0.762	2.37	0.0935	1.44	0.61	576	16

Sample and grain	Ion Beam Intensities (mV)			Concentrations		Isotope Ratios (not corrected for common Pb)									Age (Ma)		
	$^{206}\text{Pb}$	$^{207}\text{Pb}$	$^{238}\text{U}$	U (ppm)	Pb (ppm)	$\frac{^{238}\text{U}}{^{206}\text{Pb}}$	$\pm 1\sigma \%$ err	$\frac{^{207}\text{Pb}}{^{206}\text{Pb}}$	$\pm 1\sigma \%$ err	$\frac{^{207}\text{Pb}}{^{235}\text{U}}$	$\pm 1\sigma \%$ err	$\frac{^{206}\text{Pb}}{^{238}\text{U}}$	$\pm 1\sigma \%$ err	corr. coef.	$\frac{^{206}\text{Pb}}{^{238}\text{U}}$	$\pm 2\sigma$ abs	
	<b>JNC 918 (BNG SK 5146 1246) Maplewell Group, Beacon Hill Fm, Benscliffe Breccia at Pillar Rock, Massive andesite breccia and coarse grained volcaniclastic sandstone.</b>																
16	3.4	0.17	100	123	11	10.38	1.53	0.0613	2.04	0.814	2.55	0.0963	1.53	0.60	593	17	
17	0.7	0.04	11	121	11	10.53	1.68	0.0611	2.13	0.801	2.71	0.0950	1.68	0.62	585	19	
18	0.6	0.03	8	55	5	10.49	1.80	0.0573	4.22	0.754	4.59	0.0954	1.80	0.39	587	20	
19	0.6	0.03	11	75	7	10.45	1.62	0.0597	3.36	0.788	3.73	0.0957	1.62	0.43	589	18	
20	0.5	0.03	8	74	7	10.51	1.70	0.0612	2.98	0.802	3.44	0.0951	1.70	0.50	586	19	
21	0.8	0.04	12	47	4	10.38	1.73	0.0566	4.89	0.752	5.19	0.0963	1.73	0.33	593	20	
22	0.5	0.03	8	80	7	10.44	1.69	0.0565	3.07	0.746	3.51	0.0958	1.69	0.48	590	19	
23	1.1	0.07	17	121	11	10.49	1.56	0.0593	2.13	0.780	2.64	0.0954	1.56	0.59	587	17	
24	0.5	0.03	8	41	4	10.59	1.46	0.0565	5.67	0.736	5.85	0.0944	1.46	0.25	582	16	
25	0.6	0.03	9	90	7	11.32	1.44	0.0576	3.02	0.701	3.35	0.0883	1.44	0.43	546	15	
26	6.6	0.42	106	105	9	10.24	1.07	0.0594	2.30	0.799	2.53	0.0976	1.07	0.42	600	12	
27	0.6	0.03	9	140	12	10.08	1.29	0.0594	1.80	0.812	2.21	0.0992	1.29	0.58	610	15	
28	1.9	0.10	29	107	9	10.16	0.98	0.0600	2.25	0.814	2.45	0.0984	0.98	0.40	605	11	
30	1.8	0.10	29	116	10	10.22	1.10	0.0596	2.10	0.804	2.37	0.0979	1.10	0.47	602	13	
32	0.8	0.05	7	170	15	10.32	1.76	0.0609	1.52	0.814	2.33	0.0969	1.76	0.76	596	20	
33	0.9	0.06	7	89	8	10.46	1.01	0.0600	2.70	0.791	2.88	0.0956	1.01	0.35	589	11	
34	2.7	0.13	80	133	12	10.12	1.09	0.0623	2.02	0.848	2.29	0.0988	1.09	0.47	608	13	
36	3.2	0.16	96	43	4	10.50	1.14	0.0613	4.94	0.805	5.07	0.0952	1.14	0.23	586	13	
37	1.0	0.07	9	63	5	11.06	1.13	0.0593	3.97	0.740	4.12	0.0904	1.13	0.27	558	12	
40	2.7	0.13	79	60	5	10.25	1.01	0.0602	3.83	0.810	3.96	0.0976	1.01	0.26	600	12	
41	2.7	0.13	77	79	7	10.33	0.95	0.0579	3.13	0.772	3.27	0.0968	0.95	0.29	595	11	
42	0.4	0.02	7	71	6	10.16	1.09	0.0569	3.33	0.772	3.50	0.0984	1.09	0.31	605	13	
43	0.5	0.02	7	94	8	9.98	1.09	0.0592	2.63	0.818	2.85	0.1002	1.09	0.38	615	13	
44	0.3	0.02	6	63	6	10.12	1.09	0.0603	3.55	0.822	3.72	0.0988	1.09	0.29	607	13	
45	0.8	0.05	14	143	12	10.38	0.92	0.0581	1.81	0.772	2.03	0.0964	0.92	0.45	593	10	
46	0.8	0.04	12	84	7	10.14	0.99	0.0578	2.93	0.786	3.09	0.0986	0.99	0.32	606	11	
47	0.7	0.04	12	66	6	10.16	1.32	0.0566	3.67	0.768	3.90	0.0985	1.32	0.34	605	15	
48	0.3	0.02	5	69	6	10.03	0.96	0.0633	3.29	0.869	3.43	0.0997	0.96	0.28	613	11	
49	0.5	0.03	7	81	7	10.37	0.90	0.0574	3.02	0.763	3.15	0.0964	0.90	0.29	593	10	
50	0.5	0.03	7	120	11	10.06	0.89	0.0584	2.02	0.801	2.21	0.0994	0.89	0.40	611	10	

Sample and grain	Ion Beam Intensities (mV)			Concentrations		Isotope Ratios (not corrected for common Pb)								Age (Ma)		
	$^{206}\text{Pb}$	$^{207}\text{Pb}$	$^{238}\text{U}$	U (ppm)	Pb (ppm)	$\frac{^{238}\text{U}}{^{206}\text{Pb}}$	$\pm 1\sigma$ % err	$\frac{^{207}\text{Pb}}{^{206}\text{Pb}}$	$\pm 1\sigma$ % err	$\frac{^{207}\text{Pb}}{^{235}\text{U}}$	$\pm 1\sigma$ % err	$\frac{^{206}\text{Pb}}{^{238}\text{U}}$	$\pm 1\sigma$ % err	corr. coef.	$\frac{^{206}\text{Pb}}{^{238}\text{U}}$	$\pm 2\sigma$ abs
<b>JNC 918 (BNG SK 5146 1246) Maplewell Group, Beacon Hill Fm, Benscliffe Breccia at Pillar Rock, Massive andesite breccia and coarse grained volcaniclastic sandstone.</b>																
51	0.3	0.02	5	51	4	10.50	1.19	0.0567	4.65	0.744	4.80	0.0952	1.19	0.25	586	13
55	0.7	0.04	12	57	5	10.10	0.98	0.0600	3.96	0.820	4.08	0.0990	0.98	0.24	609	11
56	0.2	0.01	4	175	15	10.23	0.91	0.0592	1.49	0.798	1.75	0.0977	0.91	0.52	601	10
57	0.5	0.03	9	311	27	10.61	0.94	0.0592	0.93	0.769	1.32	0.0943	0.94	0.71	581	10
58	1.0	0.07	9	75	7	10.31	1.05	0.0594	3.07	0.795	3.25	0.0970	1.05	0.32	597	12
59	1.0	0.07	9	63	6	10.18	0.93	0.0613	3.55	0.830	3.67	0.0982	0.93	0.25	604	11
61	1.1	0.07	9	138	12	10.38	1.14	0.0590	1.87	0.784	2.19	0.0964	1.14	0.52	593	13
62	1.1	0.07	9	87	7	10.35	1.09	0.0590	2.80	0.786	3.01	0.0966	1.09	0.36	595	12
63	1.0	0.07	9	319	28	10.19	0.89	0.0612	1.13	0.827	1.43	0.0981	0.89	0.62	603	10
64	2.6	0.13	75	79	7	10.32	1.00	0.0591	2.98	0.790	3.14	0.0969	1.00	0.32	596	11
65	2.5	0.13	74	48	4	10.25	1.07	0.0593	4.63	0.798	4.75	0.0976	1.07	0.23	600	12
66	2.5	0.12	72	78	7	10.23	1.03	0.0606	2.95	0.817	3.13	0.0978	1.03	0.33	601	12
67	2.7	0.13	79	76	7	10.08	0.97	0.0579	3.04	0.793	3.20	0.0992	0.97	0.30	610	11
68	2.7	0.13	79	123	10	10.79	0.93	0.0585	2.16	0.747	2.35	0.0927	0.93	0.39	571	10
69	2.5	0.12	73	65	6	10.35	0.94	0.0605	3.48	0.806	3.60	0.0966	0.94	0.26	595	11
70	1.0	0.08	9	204	18	10.36	0.91	0.0590	1.31	0.786	1.59	0.0966	0.91	0.57	594	10
72	0.9	0.07	8	81	7	10.16	1.03	0.0592	2.92	0.803	3.10	0.0984	1.03	0.33	605	12
73	2.4	0.13	71	101	9	10.14	1.00	0.0595	2.40	0.809	2.60	0.0986	1.00	0.38	606	12
75	2.3	0.13	68	115	10	10.11	0.92	0.0611	2.06	0.834	2.26	0.0989	0.92	0.41	608	11
77	1.0	0.07	8	70	6	10.28	0.94	0.0600	3.33	0.805	3.46	0.0973	0.94	0.27	599	11

**JNC 846 (BNG SK 5244 1502) Maplewell Group, Hanging Rocks Fm, medium grained poorly sorted micaceous sandstone.**

1	0.8	0.05	12	144	14	9.66	1.22	0.0592	1.88	0.845	2.24	0.1035	1.22	0.54	635	15
2	0.6	0.03	9	105	10	10.01	1.51	0.0588	2.55	0.810	2.97	0.0999	1.51	0.51	614	18
3	0.8	0.05	13	158	14	10.18	1.21	0.0609	2.26	0.825	2.56	0.0982	1.21	0.47	604	14
4	0.9	0.05	13	161	15	9.93	1.33	0.0599	1.73	0.831	2.18	0.1007	1.33	0.61	618	16
5	1.5	0.08	23	272	25	9.96	1.10	0.0610	1.11	0.845	1.57	0.1004	1.10	0.71	617	13
7	0.6	0.03	9	107	10	10.06	1.22	0.0601	2.52	0.823	2.80	0.0994	1.22	0.44	611	14
8	0.8	0.04	12	146	13	10.07	1.23	0.0603	1.90	0.826	2.26	0.0993	1.23	0.54	610	14

Sample and grain	Ion Beam Intensities (mV)			Concentrations		Isotope Ratios (not corrected for common Pb)									Age (Ma)	
	$^{206}\text{Pb}$	$^{207}\text{Pb}$	$^{238}\text{U}$	U (ppm)	Pb (ppm)	$\frac{^{238}\text{U}}{^{206}\text{Pb}}$	$\pm 1\sigma$ % err	$\frac{^{207}\text{Pb}}{^{206}\text{Pb}}$	$\pm 1\sigma$ % err	$\frac{^{207}\text{Pb}}{^{235}\text{U}}$	$\pm 1\sigma$ % err	$\frac{^{206}\text{Pb}}{^{238}\text{U}}$	$\pm 1\sigma$ % err	corr. coef.	$\frac{^{206}\text{Pb}}{^{238}\text{U}}$	$\pm 2\sigma$ abs
<b>JNC 846 (BNG SK 5244 1502) Maplewell Group, Hanging Rocks Fm, medium grained poorly sorted micaceous sandstone.</b>																
9	0.6	0.03	9	110	10	10.13	1.10	0.0601	2.47	0.818	2.70	0.0987	1.10	0.41	607	13
10	1.3	0.07	20	240	22	10.04	1.15	0.0610	1.22	0.837	1.68	0.0996	1.15	0.68	612	13
11	0.8	0.05	13	152	14	10.00	1.19	0.0604	1.86	0.833	2.21	0.1000	1.19	0.54	614	14
12	0.4	0.02	6	73	7	10.06	1.24	0.0593	3.55	0.813	3.76	0.0994	1.24	0.33	611	14
13	0.6	0.03	9	105	10	9.84	1.34	0.0614	2.50	0.861	2.84	0.1016	1.34	0.47	624	16
15	0.4	0.03	7	81	7	10.36	1.61	0.0644	3.08	0.856	3.48	0.0965	1.61	0.46	594	18
16	0.6	0.03	8	95	10	9.09	1.50	0.0617	2.49	0.936	2.91	0.1101	1.50	0.52	673	19
18	0.7	0.04	12	143	13	10.30	1.41	0.0607	1.98	0.813	2.43	0.0971	1.41	0.58	598	16
19	1.2	0.07	11	227	20	10.04	1.44	0.0599	1.33	0.823	1.96	0.0996	1.44	0.73	612	17
20	0.8	0.05	8	152	14	9.93	1.24	0.0594	1.84	0.826	2.22	0.1007	1.24	0.56	619	15
21	0.4	0.02	12	80	7	10.01	1.22	0.0592	3.33	0.816	3.55	0.0999	1.22	0.34	614	14
23	0.7	0.04	17	125	11	10.10	1.30	0.0597	2.29	0.815	2.63	0.0990	1.30	0.49	608	15
24	0.3	0.02	8	64	6	10.17	1.18	0.0585	4.04	0.794	4.21	0.0984	1.18	0.28	605	14
25	0.7	0.04	9	135	12	10.04	1.19	0.0606	2.06	0.833	2.38	0.0996	1.19	0.50	612	14
26	1.0	0.05	106	186	16	10.24	1.16	0.0610	1.74	0.821	2.10	0.0977	1.16	0.56	601	13
27	1.0	0.06	9	198	17	10.48	1.16	0.0609	1.54	0.802	1.93	0.0954	1.16	0.60	588	13
28	0.4	0.02	29	79	7	10.11	1.14	0.0601	3.35	0.819	3.54	0.0989	1.14	0.32	608	13
29	0.5	0.03	29	105	9	10.42	1.28	0.0604	2.70	0.799	2.99	0.0959	1.28	0.43	591	14
30	0.9	0.15	29	36	16	2.08	1.27	0.1696	0.67	11.267	1.44	0.4817	1.27	0.89	2535	53
31	2.2	0.16	7	198	36	4.89	1.14	0.0816	0.61	2.302	1.29	0.2045	1.14	0.88	1200	25
32	0.6	0.04	7	115	10	10.23	1.24	0.0630	2.44	0.849	2.74	0.0977	1.24	0.45	601	14
33	1.7	0.20	7	84	29	2.67	1.47	0.1301	0.51	6.717	1.55	0.3745	1.47	0.94	2050	51
34	0.4	0.02	80	70	6	10.43	1.23	0.0584	3.96	0.772	4.15	0.0959	1.23	0.30	590	14
35	0.6	0.07	78	30	10	2.65	1.48	0.1309	1.22	6.806	1.92	0.3770	1.48	0.77	2062	52
36	0.5	0.03	96	95	9	9.89	1.23	0.0595	2.83	0.829	3.08	0.1011	1.23	0.40	621	14
37	0.5	0.03	9	101	9	9.90	1.22	0.0639	2.50	0.890	2.78	0.1010	1.22	0.44	620	14
38	1.8	0.11	9	276	31	8.17	1.15	0.0637	0.89	1.075	1.45	0.1225	1.15	0.79	745	16
40	1.0	0.05	79	179	16	9.94	1.14	0.0601	1.61	0.834	1.98	0.1006	1.14	0.58	618	13
41	0.8	0.05	79	145	13	9.90	1.24	0.0648	2.11	0.903	2.45	0.1010	1.24	0.51	620	15
42	0.6	0.03	77	108	9	10.36	1.21	0.0591	2.64	0.787	2.90	0.0966	1.21	0.42	594	14

Sample and grain	Ion Beam Intensities (mV)			Concentrations		Isotope Ratios (not corrected for common Pb)									Age (Ma)	
	$^{206}\text{Pb}$	$^{207}\text{Pb}$	$^{238}\text{U}$	U (ppm)	Pb (ppm)	$\frac{^{238}\text{U}}{^{206}\text{Pb}}$	$\pm 1\sigma$ % err	$\frac{^{207}\text{Pb}}{^{206}\text{Pb}}$	$\pm 1\sigma$ % err	$\frac{^{207}\text{Pb}}{^{235}\text{U}}$	$\pm 1\sigma$ % err	$\frac{^{206}\text{Pb}}{^{238}\text{U}}$	$\pm 1\sigma$ % err	corr. coef.	$\frac{^{206}\text{Pb}}{^{238}\text{U}}$	$\pm 2\sigma$ abs
<b>JNC 846 (BNG SK 5244 1502) Maplewell Group, Hanging Rocks Fm, medium grained poorly sorted micaceous sandstone.</b>																
43	0.8	0.05	7	160	14	10.37	1.18	0.0595	1.89	0.791	2.23	0.0964	1.18	0.53	593	13
44	2.1	0.12	7	390	35	9.95	1.13	0.0613	0.81	0.848	1.39	0.1005	1.13	0.81	617	13
45	1.7	0.21	6	84	29	2.59	1.17	0.1335	0.51	7.095	1.27	0.3854	1.17	0.92	2101	42
46	12.8	1.55	14	676	216	2.82	1.11	0.1306	0.16	6.378	1.13	0.3541	1.11	0.99	1954	37
47	1.0	0.06	12	192	17	10.14	1.29	0.0609	1.53	0.828	2.00	0.0986	1.29	0.64	606	15
48	0.6	0.04	12	120	11	10.20	1.26	0.0608	2.33	0.822	2.65	0.0980	1.26	0.48	603	14
49	2.8	0.17	5	438	47	8.40	1.09	0.0648	0.60	1.063	1.25	0.1190	1.09	0.87	725	15
50	1.7	0.10	7	341	29	10.44	1.18	0.0607	0.95	0.802	1.52	0.0958	1.18	0.78	590	13
52	0.5	0.03	7	86	8	9.84	1.19	0.0590	3.08	0.826	3.30	0.1016	1.19	0.36	624	14
54	3.7	0.20	8	761	62	11.10	1.14	0.0591	0.52	0.734	1.25	0.0901	1.14	0.91	556	12
55	1.4	0.08	12	221	23	8.48	1.19	0.0653	1.11	1.061	1.62	0.1179	1.19	0.73	718	16
56	0.7	0.04	4	142	13	10.27	1.21	0.0602	2.05	0.808	2.37	0.0974	1.21	0.51	599	14
58	1.3	0.08	9	273	22	11.14	1.25	0.0630	1.35	0.780	1.84	0.0898	1.25	0.68	554	13
59	0.6	0.04	9	115	10	10.34	1.46	0.0634	2.40	0.845	2.81	0.0968	1.46	0.52	595	17
60	0.2	0.01	9	35	3	10.74	1.19	0.0625	7.09	0.801	7.19	0.0931	1.19	0.17	574	13
63	5.9	0.56	9	389	99	3.54	1.29	0.1043	0.22	4.060	1.31	0.2822	1.29	0.99	1602	37
66	0.5	0.03	72	101	9	10.28	1.17	0.0595	2.73	0.798	2.97	0.0972	1.17	0.39	598	13
67	0.9	0.05	79	168	15	10.21	1.16	0.0616	1.70	0.831	2.06	0.0979	1.16	0.56	602	13
69-1 core	2.3	0.24	79	146	39	3.36	1.35	0.1097	0.45	4.501	1.43	0.2977	1.35	0.95	1680	40
69-2 rim	0.6	0.03	73	120	10	10.96	1.19	0.0621	2.43	0.782	2.70	0.0912	1.19	0.44	563	13
70	5.5	0.95	9	201	93	1.95	1.26	0.1858	0.17	13.111	1.27	0.5117	1.26	0.99	2664	55
71	3.1	0.35	9	176	53	3.08	1.34	0.1226	0.32	5.488	1.38	0.3246	1.34	0.97	1812	42
72	1.0	0.06	8	198	17	10.32	1.26	0.0582	1.65	0.778	2.08	0.0969	1.26	0.61	596	14
73	0.5	0.03	71	98	8	10.69	1.40	0.0574	3.06	0.741	3.37	0.0936	1.40	0.41	577	15
74	0.6	0.03	68	109	10	9.83	1.42	0.0573	2.57	0.804	2.94	0.1017	1.42	0.49	625	17
75	2.4	0.18	68	232	41	5.13	1.26	0.0794	0.57	2.136	1.38	0.1950	1.26	0.91	1149	26
77	0.8	0.05	8	157	14	10.06	1.43	0.0631	2.34	0.865	2.74	0.0994	1.43	0.52	611	17
78	0.8	0.05	8	161	14	10.21	1.21	0.0576	1.93	0.778	2.28	0.0979	1.21	0.53	602	14
79	0.9	0.05	67	175	16	10.14	1.17	0.0575	1.74	0.782	2.10	0.0986	1.17	0.56	606	14
80	2.4	0.14	68	466	40	10.32	1.14	0.0607	0.77	0.811	1.38	0.0969	1.14	0.83	596	13
81	0.5	0.03	69	95	9	10.16	1.21	0.0571	2.99	0.775	3.22	0.0984	1.21	0.38	605	14

Sample and grain	Ion Beam Intensities (mV)			Concentrations		Isotope Ratios (not corrected for common Pb)						Age (Ma) $\frac{^{206}\text{Pb}}{^{238}\text{U}}$	$\pm 2\sigma$ abs			
	$^{206}\text{Pb}$	$^{207}\text{Pb}$	$^{238}\text{U}$	U (ppm)	Pb (ppm)	$\frac{^{238}\text{U}}{^{206}\text{Pb}}$	$\pm 1\sigma \%$ err	$\frac{^{207}\text{Pb}}{^{206}\text{Pb}}$	$\pm 1\sigma \%$ err	$\frac{^{207}\text{Pb}}{^{235}\text{U}}$	$\pm 1\sigma \%$ err	$\frac{^{206}\text{Pb}}{^{238}\text{U}}$	$\pm 1\sigma \%$ err	corr. coef.		
<b>JNC 846 (BNG SK 5244 1502) Maplewell Group, Hanging Rocks Fm, medium grained poorly sorted micaceous sandstone.</b>																
82	0.8	0.04	10	170	14	11.18	1.38	0.0593	2.21	0.732	2.60	0.0895	1.38	0.53	552	15
83	0.7	0.04	14	142	12	10.20	1.21	0.0585	2.11	0.791	2.43	0.0980	1.21	0.50	603	14
84	0.4	0.02	11	70	6	10.01	1.38	0.0552	3.95	0.761	4.19	0.0999	1.38	0.33	614	16
85	1.1	0.07	6	198	18	9.71	1.42	0.0658	1.49	0.934	2.06	0.1030	1.42	0.69	632	17
86	1.4	0.09	11	224	24	8.34	1.29	0.0656	1.15	1.085	1.73	0.1199	1.29	0.75	730	18
87	0.9	0.08	5	75	16	4.29	1.75	0.0947	1.13	3.041	2.08	0.2330	1.75	0.84	1350	43

384 **Table DR 2.** CA-ID-TIMS U-Pb isotope data.

Sample	Compositional Parameters					Radiogenic Isotope Ratios							Isotopic Ages								
	$\frac{\text{Th}}{\text{U}}$	$^{206}\text{Pb}^*$ $\times 10^{-13}$ mol	mol % $^{206}\text{Pb}^*$	$\frac{\text{Pb}^*}{\text{Pb}_c}$	$\frac{\text{Pb}_c}{\text{pg}}$	$\frac{^{206}\text{Pb}}{^{204}\text{Pb}}$	$\frac{^{208}\text{Pb}}{^{206}\text{Pb}}$	$\frac{^{207}\text{Pb}}{^{206}\text{Pb}}$	% err	$\frac{^{207}\text{Pb}}{^{235}\text{U}}$	% err	$\frac{^{206}\text{Pb}}{^{238}\text{U}}$	% err	corr. coeff.	$\frac{^{207}\text{Pb}}{^{206}\text{Pb}}$	±	$\frac{^{207}\text{Pb}}{^{235}\text{U}}$	±	$\frac{^{206}\text{Pb}}{^{238}\text{U}}$	±	
	(a)	(b)	(c)	(d)	(e)	(d)	(e)	(d)	(e)	(d)	(e)	(d)	(e)	(f)	(g)	(f)	(g)	(f)	(g)	(f)	(g)
<b>JNC 916 (BNG SK 4766 1787) Blackbrook Group, Ives Head Fm, Morley Quarry, volcanioclastic turbidite, coarse to medium grained volcanioclastic sandstone bed.</b>																					
916-1	0.818	0.9041	97.68%	14	1.78	784	0.254	0.060311	0.399	0.832198	0.474	0.100121	0.139	0.647	613.50	8.62	614.83	2.19	615.19	0.81	
916-2	0.772	0.8731	98.96%	31	0.76	1747	0.240	0.060361	0.195	0.832210	0.268	0.100039	0.104	0.796	615.31	4.21	614.84	1.23	614.71	0.61	
916-3	1.015	1.7281	99.25%	45	1.08	2424	0.316	0.060354	0.164	0.832966	0.237	0.100142	0.101	0.823	615.08	3.55	615.26	1.09	615.31	0.59	
916-4	1.200	1.2275	99.33%	53	0.68	2727	0.372	0.060364	0.160	0.839782	0.238	0.100944	0.115	0.810	615.47	3.46	619.03	1.10	620.00	0.68	
916-5	0.870	4.9560	99.68%	102	1.33	5643	0.270	0.060299	0.101	0.830639	0.186	0.099954	0.097	0.939	613.08	2.18	613.97	0.86	614.21	0.57	
916-6	0.776	0.9826	98.95%	30	0.87	1727	0.244	0.061388	0.199	0.857714	0.269	0.101380	0.097	0.809	651.64	4.28	628.87	1.26	622.56	0.57	
916-7	0.809	0.9824	98.90%	29	0.91	1656	0.252	0.060361	0.205	0.829311	0.275	0.099691	0.096	0.806	615.30	4.44	613.23	1.27	<b>612.67</b>	<b>0.56</b>	
916-8	0.776	0.7048	98.50%	21	0.89	1215	0.242	0.060454	0.260	0.829855	0.335	0.099602	0.120	0.734	618.63	5.61	613.53	1.54	<b>612.15</b>	<b>0.70</b>	
916-9	0.690	1.3007	99.32%	47	0.74	2687	0.215	0.060354	0.145	0.830851	0.224	0.099887	0.104	0.862	615.05	3.12	614.08	1.03	<b>613.82</b>	<b>0.61</b>	
916-10	1.066	0.9138	99.16%	41	0.64	2178	0.327	0.059382	0.187	0.818128	0.260	0.099968	0.104	0.800	579.91	4.06	607.00	1.19	614.29	0.61	
916-11	0.718	0.8734	99.05%	33	0.69	1919	0.223	0.060378	0.182	0.831247	0.257	0.099895	0.104	0.816	615.91	3.94	614.30	1.18	<b>613.87</b>	<b>0.61</b>	
<b>JNC 836 (BNG SK 4772 1700), Blackbrook Group, Ives Head Fm at Ives Head, turbidite bed, volcanioclastic sandstone.</b>																					
836-1	0.810	4.9699	99.73%	120	1.12	6708	0.252	0.060308	0.174	0.832253	0.228	0.100133	0.099	0.701	613.40	3.76	614.86	1.05	615.26	0.58	
836-2	0.804	4.6447	99.57%	75	1.67	4214	0.250	0.060335	0.128	0.833300	0.212	0.100213	0.114	0.859	614.38	2.77	615.44	0.98	615.73	0.67	
836-3	1.101	0.7845	97.66%	15	1.56	778	0.342	0.060380	0.401	0.842139	0.477	0.101202	0.140	0.647	616.01	8.66	620.33	2.22	621.51	0.83	
836-4	1.033	1.3642	98.44%	22	1.79	1168	0.321	0.060339	0.286	0.830166	0.358	0.099831	0.122	0.700	614.53	6.18	613.70	1.65	613.48	0.71	
836-5	0.900	3.6772	99.77%	146	0.70	7970	0.280	0.060311	0.098	0.833126	0.179	0.100232	0.091	0.943	613.53	2.12	615.35	0.83	615.84	0.53	
836-6	0.790	7.9385	99.81%	173	1.23	9733	0.246	0.060365	0.091	0.828011	0.177	0.099528	0.095	0.953	615.45	1.96	612.51	0.81	<b>611.71</b>	<b>0.55</b>	
836-7	0.757	1.8113	99.07%	35	1.40	1967	0.236	0.060336	0.176	0.828618	0.248	0.099648	0.098	0.831	614.41	3.79	612.85	1.14	<b>612.42</b>	<b>0.57</b>	
836-8	0.873	1.8599	99.30%	47	1.08	2613	0.272	0.060457	0.152	0.831118	0.226	0.099749	0.096	0.859	618.74	3.28	614.23	1.04	<b>613.01</b>	<b>0.56</b>	
836-9	0.938	0.9852	99.32%	49	0.56	2667	0.292	0.060289	0.149	0.830135	0.224	0.099909	0.096	0.864	612.74	3.22	613.69	1.03	613.94	0.56	
836-10	0.845	1.0035	99.49%	64	0.43	3535	0.263	0.060355	0.134	0.830210	0.214	0.099809	0.104	0.870	615.10	2.89	613.73	0.99	<b>613.36</b>	<b>0.61</b>	
<b>JNC 917 (BNG SK 4637 1712) Blackbrook Group, Ives Head Fm, South Quarry Breccia, volcanioclastic sandstone and mudstone breccia.</b>																					
917-1	0.818	1.3654	98.88%	29	1.28	1632	0.255	0.060421	0.218	0.830881	0.287	0.099781	0.099	0.782	617.43	4.71	614.10	1.32	<b>613.20</b>	<b>0.58</b>	
917-2	0.888	1.3073	99.19%	41	0.89	2247	0.276	0.060311	0.163	0.826647	0.237	0.099454	0.097	0.845	613.50	3.53	611.75	1.09	<b>611.28</b>	<b>0.57</b>	
917-3	0.837	0.7527	98.80%	27	0.76	1522	0.261	0.060476	0.223	0.834390	0.292	0.100111	0.099	0.784	619.40	4.82	616.05	1.35	615.13	0.58	

Sample	Compositional Parameters						Radiogenic Isotope Ratios								Isotopic Ages						
	$\frac{\text{Th}}{\text{U}}$	$^{206}\text{Pb}^*$ $\times 10^{-13}$ mol	mol %	$\frac{\text{Pb}^*}{^{206}\text{Pb}^*}$	$\text{Pb}_c$	$\frac{^{206}\text{Pb}}{^{204}\text{Pb}}$	$\frac{^{208}\text{Pb}}{^{206}\text{Pb}}$	$\frac{^{207}\text{Pb}}{^{206}\text{Pb}}$	% err	$\frac{^{207}\text{Pb}}{^{235}\text{U}}$	% err	$\frac{^{206}\text{Pb}}{^{238}\text{U}}$	% err	corr. coef.	$\frac{^{207}\text{Pb}}{^{206}\text{Pb}}$	±	$\frac{^{207}\text{Pb}}{^{235}\text{U}}$	±	$\frac{^{206}\text{Pb}}{^{238}\text{U}}$	±	
	(a)	(b)	(c)	(d)	(e)	(f)	(g)	(d)	(e)	(d)	(e)	(d)	(e)	(f)	(g)	(f)	(g)	(f)	(g)	(f)	(g)
<b>JNC 917 (BNG SK 4637 1712) Blackbrook Group, Ives Head Fm, South Quarry Breccia, volcanioclastic sandstone and mudstone breccia</b>																					
917-4	0.874	1.4134	98.42%	21	1.88	1151	0.272	0.060369	0.265	0.830974	0.336	0.099877	0.109	0.744	615.61	5.73	614.15	1.55	<b>613.76</b>	<b>0.64</b>	
917-5	0.804	3.3230	99.75%	132	0.68	7394	0.250	0.060383	0.098	0.830544	0.183	0.099802	0.096	0.939	616.09	2.12	613.91	0.84	<b>613.32</b>	<b>0.56</b>	
917-6	0.758	1.4526	98.96%	31	1.26	1756	0.236	0.060328	0.208	0.829462	0.279	0.099764	0.104	0.781	614.10	4.49	613.31	1.28	<b>613.10</b>	<b>0.61</b>	
917-7	0.996	0.3395	97.21%	12	0.81	653	0.310	0.060479	0.438	0.834828	0.520	0.100158	0.145	0.658	619.55	9.46	616.29	2.40	615.40	0.85	
917-8	1.029	0.8713	97.70%	15	1.70	791	0.319	0.060243	0.352	0.833103	0.426	0.100343	0.104	0.771	611.09	7.60	615.33	1.96	616.49	0.61	
917-9	0.958	0.5610	98.69%	25	0.62	1389	0.297	0.060337	0.244	0.835428	0.316	0.100467	0.116	0.734	614.45	5.28	616.62	1.46	617.21	0.68	
917-10	1.181	1.2504	99.27%	49	0.76	2507	0.367	0.060370	0.149	0.837311	0.223	0.100637	0.092	0.873	615.69	3.22	617.66	1.03	618.20	0.54	
<b>JNC 918 (BNG SK 5146 1246) Maplewell Group, Beacon Hill Fm, Benscliffe Breccia at Pillar Rock, Massive andesite breccia and coarse grained volcanioclastic sandstone.</b>																					
918-1	0.813	1.5478	98.91%	30	1.42	1665	0.253	0.060400	0.263	0.831346	0.337	0.099871	0.150	0.662	616.69	5.68	614.36	1.56	613.73	0.88	
918-2	0.823	0.2736	90.82%	3	2.30	198	0.258	0.059363	1.360	.751061	0.542	.091802	0.275	0.710	579.16	29.55	568.84	6.71	566.26	0.49	
918-3	0.600	0.5695	97.34%	11	1.29	684	0.187	0.059168	0.436	.752816	0.522	.092320	0.132	0.727	571.98	9.48	569.86	2.28	<b>569.32</b>	<b>0.72</b>	
918-4	0.490	0.7836	99.46%	55	0.36	3349	0.153	0.059269	0.126	.755601	0.220	.092504	0.119	0.890	575.67	2.75	571.47	0.96	<b>570.41</b>	<b>0.65</b>	
918-5	1.155	0.3340	98.61%	25	0.39	1308	0.359	0.060167	0.281	.824720	0.374	.099459	0.169	0.709	608.38	6.07	610.68	1.72	611.30	0.99	
918-6	0.841	0.8034	99.04%	34	0.64	1904	0.262	0.059104	0.188	.751434	0.267	.092250	0.111	0.809	569.67	4.10	569.06	1.16	<b>568.90</b>	<b>0.60</b>	
918-7	0.942	1.1857	96.79%	10	3.28	562	0.292	0.060022	0.551	0.826189	0.637	0.099876	0.160	0.629	603.16	11.92	611.50	2.93	613.75	0.94	
918-8	0.770	1.1994	99.01%	32	0.99	1839	0.239	0.060189	0.220	0.831416	0.290	0.100230	0.103	0.779	609.13	4.75	614.40	1.34	615.83	0.61	
918-9	0.613	0.6635	98.23%	17	0.99	1025	0.190	0.060383	0.301	0.835880	0.386	0.100444	0.138	0.726	616.08	6.50	616.87	1.78	617.09	0.81	
918-10	1.006	0.4393	97.93%	16	0.77	879	0.314	0.060534	0.515	0.832075	0.598	0.099738	0.156	0.627	621.49	11.11	614.76	2.76	612.94	0.91	
918-11	1.025	0.8994	98.57%	24	1.08	1273	0.319	0.060325	0.253	0.830539	0.329	0.099898	0.111	0.772	614.04	5.48	613.91	1.52	613.88	0.65	
<b>JNC 911 (BNG SK 5091 1488) Maplewell Group, Beacon Hill Fm, Beacon Tuff member, fine grained vitric tuff</b>																					
911-1	0.853	0.2204	97.00%	11	0.57	608	0.266	0.060382	0.551	0.830848	0.624	0.099841	0.167	0.548	616.05	11.89	614.08	2.88	613.55	0.98	
911-2	0.959	0.2888	98.70%	26	0.31	1404	0.300	0.060748	0.362	0.836241	0.436	0.099883	0.163	0.601	629.12	7.81	617.07	2.02	613.79	0.95	
911-3	0.728	0.3385	98.21%	18	0.51	1015	0.227	0.060593	0.515	0.830965	0.584	0.099507	0.163	0.539	623.57	11.11	614.15	2.69	611.59	0.95	
911-4	0.892	0.8723	99.15%	39	0.62	2154	0.277	0.060355	0.203	0.832170	0.267	0.100045	0.106	0.727	615.08	4.39	614.82	1.23	614.74	0.62	

Sample	Compositional Parameters						Radiogenic Isotope Ratios								Isotopic Ages						
	Th U	$^{206}\text{Pb}^*$ $\times 10^{-13}$ mol	mol % $^{206}\text{Pb}^*$	$\frac{\text{Pb}^*}{\text{Pb}_c}$	$\text{Pb}_c$ (pg)	$\frac{^{206}\text{Pb}}{^{204}\text{Pb}}$	$\frac{^{208}\text{Pb}}{^{206}\text{Pb}}$	$\frac{^{207}\text{Pb}}{^{206}\text{Pb}}$	% err	$\frac{^{207}\text{Pb}}{^{235}\text{U}}$	% err	$\frac{^{206}\text{Pb}}{^{238}\text{U}}$	% err	corr. coef.	$\frac{^{207}\text{Pb}}{^{206}\text{Pb}}$	±	$\frac{^{207}\text{Pb}}{^{235}\text{U}}$	±	$\frac{^{206}\text{Pb}}{^{238}\text{U}}$	±	
	(a)	(b)	(c)	(d)	(d)	(e)	(d)	(e)	(d)	(e)	(d)	(e)	(f)	(g)	(f)	(g)	(f)	(g)	(f)	(g)	
<b>JNC 907 (BNG SK 4572 1289) Maplewell Group, Bradgate Fm, Bardon Hill Quarry, volcaniclastic sandstone-siltstone.</b>																					
907-1	0.728	1.0034	99.57%	74	0.36	4250	0.227	0.059034	0.121	0.745624	0.197	0.091645	0.091	0.907	567.08	2.63	565.68	0.86	<b>565.34</b>	<b>0.49</b>	
907-2	1.381	0.5476	99.00%	37	0.46	1828	0.430	0.060407	0.191	0.832527	0.264	0.100000	0.110	0.781	617.03	4.13	615.01	1.22	614.46	0.64	
907-3	0.786	0.1982	98.29%	19	0.29	1065	0.245	0.059038	0.322	0.747964	0.405	0.091928	0.151	0.680	567.21	7.02	567.04	1.76	<b>567.00</b>	<b>0.82</b>	
907-4	0.526	0.9329	99.53%	65	0.36	3884	0.164	0.059039	0.124	0.746907	0.200	0.091795	0.091	0.900	567.24	2.71	566.43	0.87	<b>566.23</b>	<b>0.49</b>	
907-5	0.988	0.8248	99.21%	43	0.54	2313	0.308	0.059072	0.168	0.745812	0.247	0.091609	0.088	0.931	568.51	3.66	565.79	1.07	<b>565.11</b>	<b>0.47</b>	
<b>JNC 912 (BNG SK 4860 1095) Maplewell Group, Bradgate Fm, Park Breccia, medium grained volcaniclastic sandstone with mudstone rafts.</b>																					
912-1	0.958	1.7591	96.41%	9	5.47	500	0.299	0.059189	0.364	0.745734	0.444	0.091419	0.157	0.641	572.80	7.91	565.75	1.92	563.99	0.85	
912-2	0.975	1.4672	98.19%	18	2.24	1004	0.304	0.059074	0.269	0.743811	0.340	0.091360	0.095	0.803	568.59	5.86	564.63	1.47	563.65	0.51	
912-3	0.959	1.1188	96.53%	9	3.35	519	0.299	0.059012	0.381	0.741328	0.479	0.091151	0.188	0.664	566.29	8.30	563.18	2.07	<b>562.41</b>	<b>1.01</b>	
912-4	0.897	0.3926	99.20%	41	0.26	2283	0.279	0.060394	0.211	0.832673	0.289	0.100040	0.135	0.737	616.50	4.55	615.09	1.34	614.71	0.79	
912-5	0.739	0.3679	99.22%	41	0.24	2337	0.230	0.060321	0.254	0.828301	0.325	0.099635	0.130	0.686	613.88	5.48	612.67	1.49	612.34	0.76	
912-6	0.645	0.1324	98.08%	16	0.22	946	0.200	0.060141	0.415	0.827562	0.556	0.099845	0.300	0.679	607.39	8.98	612.26	2.56	613.58	1.76	
912-7	0.925	0.9862	90.88%	3	8.27	196	0.288	0.058757	0.636	0.737863	0.718	0.091119	0.188	0.545	556.85	13.86	561.16	3.10	<b>562.22</b>	<b>1.01</b>	
912-8	0.841	0.4506	97.70%	14	0.88	792	0.262	0.058822	0.416	0.737648	0.486	0.090993	0.128	0.639	559.22	9.07	561.03	2.09	<b>561.48</b>	<b>0.69</b>	
912-9	0.968	1.1579	99.62%	90	0.36	4832	0.302	0.058948	0.142	0.740356	0.214	0.091130	0.103	0.826	563.94	3.08	562.61	0.93	<b>562.29</b>	<b>0.55</b>	
912-10	0.978	0.7051	99.36%	52	0.38	2830	0.305	0.058813	0.155	0.737693	0.231	0.091012	0.101	0.848	558.92	3.37	561.06	0.99	<b>561.59</b>	<b>0.54</b>	
912-11	1.020	1.3312	99.35%	52	0.73	2780	0.318	0.058897	0.221	0.738713	0.280	0.091008	0.116	0.663	562.04	4.82	561.65	1.21	<b>561.56</b>	<b>0.62</b>	
912-12	0.707	1.3966	99.60%	80	0.46	4585	0.220	0.058818	0.117	0.738201	0.221	0.091067	0.131	0.903	559.06	2.54	561.36	0.95	<b>561.92</b>	<b>0.70</b>	
912-13tk	0.921	1.3740	99.17%	40	0.95	2195	0.288	0.058953	0.396	0.738231	0.573	0.090862	0.318	0.747	564.09	8.63	561.37	2.47	<b>560.70</b>	<b>1.71</b>	
912-2tk	0.980	2.1717	99.44%	60	1.02	3236	0.306	0.058923	0.369	0.740830	0.449	0.091228	0.183	0.602	563.00	8.05	562.89	1.94	<b>562.86</b>	<b>0.99</b>	
912-3tk	0.707	0.2218	89.49%	3	2.16	173	0.218	0.060231	1.605	0.852674	2.534	0.102720	0.638	1.315	610.65	34.68	626.12	11.84	630.40	3.83	
912-4tk	1.020	1.2248	98.82%	29	1.21	1546	0.319	0.059069	0.434	0.741640	0.573	0.091102	0.216	0.756	568.40	9.44	563.36	2.48	<b>562.12</b>	<b>1.16</b>	
912-5tk	0.905	0.8641	99.01%	33	0.72	1840	0.282	0.058796	0.190	0.736851	0.515	0.090934	0.242	1.154	558.29	4.15	560.57	2.22	<b>561.13</b>	<b>1.30</b>	
912-6tk	1.025	0.5127	97.94%	16	0.89	884	0.320	0.059719	0.753	0.776568	1.084	0.094354	0.348	0.967	592.18	16.32	583.52	4.81	581.30	1.93	
912-7tk	0.820	0.6422	98.05%	16	1.06	934	0.254	0.060034	0.255	0.822386	0.674	0.099396	0.262	1.295	603.57	5.53	609.38	3.09	610.94	1.53	

Notes: (a) calculated from measured  $^{208}\text{Pb}/^{206}\text{Pb}$  assuming concordance, (b) radiogenic/common Pb in sample (c) corrected for fractionation and spike, (d) corrected for fractionation, spike and blank (Stacey and Kramers (1975), (e) uncertainty is  $\pm 2$  SE %, (f) calculated using decay constants of Jaffey et al., (1971) and  $^{238}\text{U}/^{235}\text{U}$  for crustal zircon from Hiess et al., (2013), (g) uncertainty is  $\pm 2$  SD absolute.

388 **Table DR 3.** Chemical compositions of volcanic pebbles separated from Hanging Rocks  
389 Formation conglomerate sample JNC 685. Due to the small size of each sample (3-4 grams)  
390 only a limited range of trace elements could be determined. Analysis was conducted at the  
391 BGS using a Fisons/ARL 3580 inductively-coupled plasma-atomic emission spectrometer.  
392

	JNC 685A	JNC685B	JNC685C
SiO <sub>2</sub> (wt%)	67.41	67.64	64.44
TiO <sub>2</sub>	0.22	0.51	0.52
Al <sub>2</sub> O <sub>3</sub>	17.94	18.07	18.34
Fe <sub>2</sub> O <sub>3</sub> (tot.)	2.05	1.21	4.25
MnO	0.06	0.02	0.09
MgO	0.46	0.19	1.07
CaO	0.17	0.22	0.50
Na <sub>2</sub> O	9.19	9.52	8.20
K <sub>2</sub> O	1.02	0.81	1.16
P <sub>2</sub> O <sub>5</sub>	0.00	0.03	0.03
LOI	0.72	0.83	1.37
Total	99.24	99.05	99.97
Sr (ppm)	179	196	228
Ba	357	317	429
V	27	36	91
Zn	28	15	57
Cu	9	8	12
Pb	18	21	16
Zr	185	285	258
Co	21	25	16
Y	30	42	39
La	9	5	13
Cr	4	5	6

393

## 394 REFERENCES CITED

- 395 Bauer, W., Walsh, G. J., de Waele, B., Thomas, R. J., Horstwood, M. S. A., Bracciali, L.,  
396 Schofield, D. I., Wollenberg, U., Lidke, D. J., Rasaona, I. T., and Rabarimanana, M.  
397 H., 2011, Cover sequences at the northern margin of the Antongil Craton, NE  
398 Madagascar: Precambrian Research, v. 189, p. 292-312.
- 399 Bevins, R.E., Pharaoh, T.C., Cope, J.C.W., and Brewer, T.S., 1995, Geochemical character of  
400 Neoproterozoic rocks in southwest Wales. Geological Magazine, v. 132, p. 339-349.
- 401 Boynton, H.E., and Ford, T.D., 1995, Ediacaran fossils from the Precambrian (Charnian  
402 Supergroup) of Charnwood Forest, Leicestershire, England: Mercian Geologist, v. 13,  
403 p. 165-183.

- 404 Boynton, H.E., and Moseley, J., 1999, The geology of The Brand, Charnwood Forest,  
405 Leicestershire: *Transactions of the Leicester Literary and Philosophical Society*, v. 93,  
406 p. 32-38.
- 407 Bridge, D. M., Carney, J. N., Lawley, R. S., and Rushton, A. W. A., 1998, Geology of the  
408 country around Coventry and Nuneaton. *Memoir for 1:50 000 Geological Sheet 169*  
409 (England and Wales), British Geological Survey, 185 p.
- 410 Carney, J. N., 1994, Geology of the Thringstone, Shepshed and Loughborough districts:  
411 1:10000 sheets SK 41 NW, SK 41 NE and SK 51 NW. British Geological Survey  
412 Technical Report WA/94/08, 159 p.
- 413 Carney, J.N., 1999, Revisiting the Charnian Supergroup: new advances in understanding old  
414 rocks: *Geology Today*, Nov-Dec, p. 221-229.
- 415 Carney, J.N., 2000, Igneous processes within late Precambrian volcanic centres near  
416 Whitwick, north-western Charnwood Forest: *Mercian Geologist*, v. 15, p. 7-28.
- 417 Carney, J.N., 2000b, Beacon Hill, Geological Conservation Review Series No. 20, Joint  
418 Nature Conservation Committee, Peterborough, p. 30-42.
- 419 Carney, J.N., 2000c, Outwoods-Hangingstone Hills, Geological Conservation Review Series  
420 No. 20, Joint Nature Conservation Committee, Peterborough, p. 43-48.
- 421 Carney, J. N., and Pharaoh, T. C., 2000, Bardon Hill, In Carney, J.N., Horak, J.M., Pharaoh,  
422 T.C., Gibbons, W., Wilson, D., Barclay, W.J., and Bevins, R.E. Precambrian rocks of  
423 England and Wales, Geological Conservation Review Series No. 20, Joint Nature  
424 Conservation Committee, Peterborough, p. 40-43.
- 425 Carney, J. N., and Noble, S. R., 2007, Geological setting, environment and age of the  
426 Charnwood biota: *Transactions of the Leicester Literary and Philosophical Society*, v.  
427 101, p. 49-51.

- 428 Compston, W., Wright, A. E., and Toghill, P., 2002, Dating the Late Precambrian volcanicity  
429 of England and Wales: Journal of the Geological Society [London], v. 159, p. 323-  
430 339.
- 431 Corfu, F., and Noble, S. R., 1992, Genesis of the southern Abitibi Greenstone-Belt, Superior  
432 Province, Canada - Evidence from zircon Hf isotope analyses using a single filament  
433 technique: *Geochimica et Cosmochimica Acta*, v. 56, p. 2081-2097.
- 434 Gerstenberger, H., and Haase, G., 1997, A highly effective emitter substance for mass  
435 spectrometric Pb isotope ratio determinations: *Chemical Geology*, v. 136, p. 309.
- 436 Hiess, J., Condon, D. J., McLean, N., and Noble, S. R., 2012,  $^{238}\text{U}/^{235}\text{U}$  Systematics in  
437 Terrestrial Uranium-Bearing Minerals: *Science*, v. 335, no. 6076, p. 1610-1614.
- 438 Horstwood, M. S. A., Foster, G. L., Parrish, R. R., Noble, S. R., and Nowell, G. M., 2003,  
439 Common-Pb corrected in situ U-Pb accessory mineral geochronology by LA-MC-  
440 ICP-MS: *Journal of Analytical Atomic Spectrometry*, v. 18, p. 837-846.
- 441 Jaffey, A. H., Flynn, K. F., Glendenin, L. E., Bentley, W. C., and Essling, A. M., 1971,  
442 Precision measurement of half-lives and specific of  $^{235}\text{U}$  and  $^{238}\text{U}$ : *Physics Reviews*,  
443 v. C4, p. 1889-1906.
- 444 Jackson, S.E., Pearson, N.J., Griffin, W.L., and Belousova, E.A., 2004, The application of  
445 laser ablation-inductively coupled plasma-mass spectrometry to in situ U-Pb zircon  
446 geochronology: *Chemical Geology*, v. 211, p. 47-69.
- 447 Liu, A. G., McIlroy, D., Antcliffe, J. B., and Brasier, M. D., 2011, Effaced preservation in the  
448 Ediacara biota and its implications for the early macrofossil record: *Palaeontology*, v.  
449 54, p. 607-630.
- 450 Ludwig, K. R., 2003, Isoplot 3.00. A geochronological toolkit for Microsoft Excel: Berkeley  
451 Geochronology Center Special Publication no. 4, 71p.

- 452 Ludwig, K. R., and Mundil, R., 2002, Extracting reliable U-Pb ages and errors from complex  
453 populations of zircons from Phanerozoic tuffs: *Geochimica et Cosmochimica Acta*, v.  
454 66, no. Supplement 1. The Goldschmidt Conference Abstracts, p. A463.
- 455 Mattinson, J. M., 2005, Zircon U-Pb chemical abrasion ("CA-TIMS") method: Combined  
456 annealing and multi-step partial dissolution analysis for improved precision and  
457 accuracy of zircon ages: *Chemical Geology*, v. 220, p. 47-66.
- 458 Moseley, J.B., and Ford, T.D., 1985, A stratigraphic revision of the Late Precambrian rocks  
459 of the Charnwood Forest, Leicestershire: *Mercian Geologist*, v. 10, p. 1-18.
- 460 Murphy, J. B., Fernandez-Suarez, J., Jeffries, T. E., and Strachan, R. A., 2004, U-Pb (LA-  
461 ICP-MS) dating of detrital zircons from Cambrian clastic rocks in Avalonia: erosion  
462 of a Neoproterozoic arc along the northern Gondwanan margin: *Journal of the*  
463 *Geological Society [London]*, v. 161, p. 243-254.
- 464 Noble, S. R., Tucker, R. D., and Pharaoh, T. C., 1993, Lower Paleozoic and Precambrian  
465 igneous rocks from Eastern England, and their bearing on late Ordovician closure of  
466 the Tornquist Sea - constraints from U-Pb and Nd isotopes: *Geological Magazine*, v.  
467 130, p. 835-846.
- 468 Pharaoh, T.C., and Evans, C.J., 1987, Moreley Quarry No. 1 Borehole: Geological well  
469 completion report: Investigation of the geothermal potential of the UK, British  
470 Geological Survey Report.
- 471 Pharaoh, T.C., Webb, P.C., Thorpe, R.S., and Beckinsale, R.D., 1987, Geochemical evidence  
472 for the tectonic setting of late Proterozoic volcanic suites in central England: In  
473 *Geochemistry and Mineralisation of Proterozoic volcanic suites* (eds T.C. Pharaoh,  
474 R.D. Beckinsale and D. Rickard), *Geological Society [London] Special Publication*  
475 33, p. 541-552.

- 476 Pharaoh, T.C., Merriman, R.J., Evans, J.A., Brewer, T.S., Webb, P.C. and Smith, N.J.P.,  
477 1991, Early Palaeozoic arc-related volcanism in the concealed Caledonides of  
478 southern Britain. *Annales de la Société Géologique de Belgique*, T114, p. 63-91.
- 479 Pharaoh, T. C., and Carney, J. N., 2000, Introduction to the Precambrian rocks of England  
480 and Wales., *Precambrian Rocks of England and Wales*. Geological Conservation  
481 Review Series., v. 20, p. 3-17.
- 482 Sambridge, M. S., and Compston, W., 1994, Mixture modeling of multi-component data sets  
483 with application to ion-probe zircon ages: *Earth And Planetary Science Letters*, v.  
484 128, p. 373-390.
- 485 Schmitz, M. D., and Schoene, B., 2007, Derivation of isotope ratios, errors, and error  
486 correlations for U-Pb geochronology using Pb-205-U-235-(U-233)-spiked isotope  
487 dilution thermal ionization mass spectrometric data: *Geochemistry Geophysics  
488 Geosystems*, v. 8, article no. Q08006, doi:10.1029/2006GC001492.
- 489 Schneider, J. L., Le Ruyet, A., Chanier, F., Buret, C., Ferriere, J., Proust, J. N., and Rosseel,  
490 J. B., 2001, Primary or secondary distal volcaniclastic turbidites: how to make the  
491 distinction? An example from the Miocene of New Zealand (Mahia Peninsula, North  
492 Island): *Sedimentary Geology*, v. 145, p. 1-22.
- 493 Simonetti, A., Heaman, L. M., Hartlaub, R. P., Creaser, R. A., MacHattie, T. G., and Bohm,  
494 C., 2005, U-Pb zircon dating by laser ablation-MC-ICP-MS using a new multiple ion  
495 counting Faraday collector array: *Journal of Analytical Atomic Spectrometry*, v. 20,  
496 p. 677-686.
- 497 Sláma, J., Kosler, J., Condon, D. J., Crowley, J. L., Gerdes, A., Hanchar, J. M., Horstwood,  
498 M. S. A., Morris, G. A., Nasdala, L., Norberg, N., Schaltegger, U., Schoene, B.,  
499 Tubrett, M. N., and Whitehouse, M. J., 2008, Plesovice zircon -- A new natural  
500 reference material for U-Pb and Hf isotopic microanalysis: *Chemical Geology*, v. 249,  
501 p. 1-35.

- 502 Stix, J., 1991, Subaqueous, intermediate to silicic-composition explosive volcanism: a  
503 review: *Earth-Science Reviews*, v. 31, p. 21-53.
- 504 Tucker, R. D., and Pharaoh, T. C., 1991, U-Pb zircon ages for Late Precambrian igneous  
505 rocks in southern Britain: *Journal of the Geological Society [London]*, v. 148, p. 435-  
506 443.
- 507 Wiedenbeck, M., Alle, P., Corfu, F., Griffin, W. L., Meier, M., Oberli, F., Vonquadt, A.,  
508 Roddick, J. C., and Speigel, W., 1995, 3 Natural Zircon Standards for U-Th-Pb, Lu-  
509 Hf, Trace-Element and Ree Analyses: *Geostandards Newsletter*, v. 19, p. 1-23.
- 510 Wilby, P. R., Carney, J. N., and Howe, M. P. A., 2011, A rich Ediacaran assemblage from  
511 eastern Avalonia: Evidence of early widespread diversity in the deep ocean: *Geology*,  
512 v. 39, p. 655-658.
- 513 Worssam, B. C., and Old, R. A., 1988, Geology of the country around Coalville, Memoir of  
514 the British Geological Survey, Sheet 155 (England and Wales), 161 p.